UNIVERSITY OF WEST BOHEMIA IN PILSEN
FACULTY OF MECHANICAL ENGINEERING

Study program: N 2301 Mechanical Engineering
Field of study: Design of Power Machines and Equipment

MASTER'S THESIS

Processing of primary probe data from steam turbine

Author: **Bc. Vojtěch KAISER**

Supervisor: **Prof. Ing. Václav URUBA, CSc.**

Consultant: **Ing. Kamil Sedlák, Ph.D.**

Academic year 2019/2020

Content

List of used abbreviations, signs and symbols 1
1 Introduction 3
2 Steam turbine 4
3 Measuring chain at calibration 5
4 Measuring equipment at data acquisition 7
5 Calibration 10
6 Calculation of pressures and velocity components 12
7 Nulling of the probe 13
8 Compressibility of steam 16
9 Data acquisition 17
9.1 Custom-made measuring application 18
9.2 Measurement of steam wetness 20
10 Speed of sound 23
11 Uncertainty of measurement 24
12 Statistics 28
13 Practical part 34
13.1 Task one – Steam tables and speed of sound 34
13.2 Task two – Calibration 37
13.3 Task three – Calibration equations 40
13.4 Task four – Flow parameters 44
13.5 Task five – Uncertainty of measurement 51
13.6 Task six – Statistics 54
14 Conclusion 61
15 Figures, tables, formulas 66
15.1 Figures 66
15.2 Tables 67
15.3 Formulas 68
16 References 69
17 Appendix 71

List of used abbreviations, signs and symbols

A	Area
c	Absolute velocity
C	Coverage factor
CL	Confidence level
c_2	Velocity vector
c_p	Specific isobaric heat capacity
c_{r_2}	Radial velocity component
c_{u_2}	Tangential velocity component
c_v	Specific isochoric heat capacity
c_{z_2}	Axial velocity component
D	Diameter of a particle
$Diff_{abs}$	Absolute difference of mean and median value
$Diff_{rel}$	Relative difference of mean and median value
EA, EDA	Exploratory (Data) Analysis
FS	Full Scale
$\widehat{g_1}$	Skewness
$\widehat{g_2}$	Kurtosis
h_i, i_i	Enthalpy
I	Beam intensity
k	Sturges number (number of bins)
k_{Di}	Dynamic pressure calibration coefficient
k_{D2}	Dynamic pressure calibration coefficient, 1. interval
k_{D3}	Dynamic pressure calibration coefficient, 2. interval
k_{S_i}	Static pressure calibration coefficient
k_{S2}	Static pressure calibration coefficient, 1. interval
k_{S3}	Static pressure calibration coefficient, 2. interval
$k_{\varepsilon ij}$	Calibration coefficient
L	Length of milled hole in V-2 spectrometric probe
N_v	Number of elements in unit volume
OEM	Original Equipment Manufacturer
p	Pressure
P	Order probability
p_B	Pressure p_B on the probe
p_C	Total pressure
p_D	Dynamic pressure
p_i	Arbitrary pressure
p_j	Arbitrary pressure
p_L	Pressure p_L on the probe
p_p	Pressure p_P on the probe
p_S	Static pressure
$Q\left(\frac{\pi D}{\lambda}\right)$	Coefficient of light scatter according to Mie theory
RNL	Numerical method for integral polydispersion characteristics
s	Entropy, standard deviation
s^2	Variance
SoS	Speed of sound
STD	Standard deviation
T	Temperature
u	Internal energy
u_A	Type A uncertainty

u_B	Type B uncertainty
u_C	Combined standard uncertainty
U	Expanded uncertainty
v	Specific volume
w	Relative speed, Speed of sound
x	Quality of steam, dryness
$\overline{x}$	Mean, median, mode
α	Yaw angle
γ	Surface tension
γ^0, γ^r	Ideal gas and residual part of Gibbs free energy
ε	Pitch angle
η	Kinematic viscosity
κ	Heat capacity ratio, isentropic coefficient
λ	Wavelength, thermal conductivity
μ	Dynamic viscosity
ϱ	Density
σ	Standard deviation
φ(D)	Water droplets scatter

1 Introduction

The aim of this master's thesis is to present a way to successfully measure and evaluate basic steam parameters in a real turbine. The values of the basic parameters are then used to calculate performance parameters. These are then checked against the designed parameters. How well the calculated and design parameters correspond, serve to approve or disapprove the calculation methods and equations. In case they are significantly different, adjustment in the calculation methods and development of more precise equations is necessary to reflect the reality better. The thesis is done under the auspices of Doosan Škoda Power, s.r.o.

In order to measure effectively the steam parameters, a measuring chain has to be composed. Measuring chain confines measurement of barometric pressure, temperature in the turbine, and pressure measurement from a 7-hole pressure probe.

Prior to the measurement, the probe needs to be calibrated. The calibration is done at the Doosan Škoda Power R&D Center in a wind tunnel. The probe is set into a stand's probe holder. The holder positions the probe in such way that angle α is set to 0 and the probe may rotate around the horizontal plane. The angle α equal to 0 ensures that a condition of pressure difference $p_L - p_P = 0$ is upheld. This rotation around the horizontal plane is given by angle ε. While rotating around the angle ε, pressures $p_1 - p_4$, p_L, p_P and p_B are being recorded. The pressures are then used to create calibration coefficients. Fitting coefficients dependent on the angle ε with a polynomial lead to creation of calibration equations.

Calibration equations are then used to calculate the steam incoming angle ε from the real data acquired from the turbine. The probe in the turbine cannot move around angle ε but it positions itself around angle α to comply with the pressure difference condition $p_L - p_P = 0$. Other calibration equations come in play to evaluate the distribution of static, dynamic, and total pressure over the blade height and steam velocity components.

The measuring chain in real application differs from the measuring chain of the calibration. It is more complicated, more equipment is used and the equipment is heavier. Additional probes for water content estimate in wet steam are used. Software controls the immediate development of variables so unusual values are easy to spot. A crew of three people is required to move the equipment efficiently and to control the measurement progress.

The thesis describes the reality of the measurement. Measurement date with the power plants is generally set months ahead, leaving the experimental crew no space for mistakes. The measurement is conducted under various conditions. This involves change in back pressure and performance or flow rate, resp. of the turbine. Only one of them is held constant while others change. From this range of data, we can conclude the performance and behavior of the turbine and check it against the design.

The thesis gives insight on different types of uncertainties and how they are determined. No measurement is a hundred percent correct, however, we can say with a certain confidence that the true value locates within an interval. This interval is called the confidence band.

The acquired data from the experimental measurement are the subject of study. Statistical analysis of the data is utilized to determine data reliability and conformity. Things such as

data distribution, mean values, standard deviations and checks against the normal distribution are done.

The information we are able to extract from the measurement are further used to determine other thermodynamic values, flow rate and real entering and leaving steam angles at the blading. Those new calculated values are as well compared to the designed values. If they do not match, engineers of construction and calculation departments will be notified. This feedback ensures that the numerical models for blading and the inner parts of turbines will keep developing, helping the company's competitiveness.

2 Steam turbine

History of a steam turbine dates back to 19th century. The first turbine was built by Sir Charles Algernon Parsons in England. Since then they have played a major role in electrical power generation as well as heat generation. [16]

Steam turbines are machines that convert energy of steam into useful work. The main part of any turbine is the pair of stator and rotor blades. The stator, stationary, blades convert the pressure energy of the steam into kinetic energy. Directing the steam onto the moving blade at axial direction. The rotor, moving, blades convert the kinetic energy into mechanical energy (work) which actuates the rotor to spin. The stator blades are firmly fitted to the inner casing of the turbine, reaching as close to the rotor as possible. The rotor blades are inserted into the rotor itself or rotor disks. The blades gradually increase in length as the steam expands. [16]

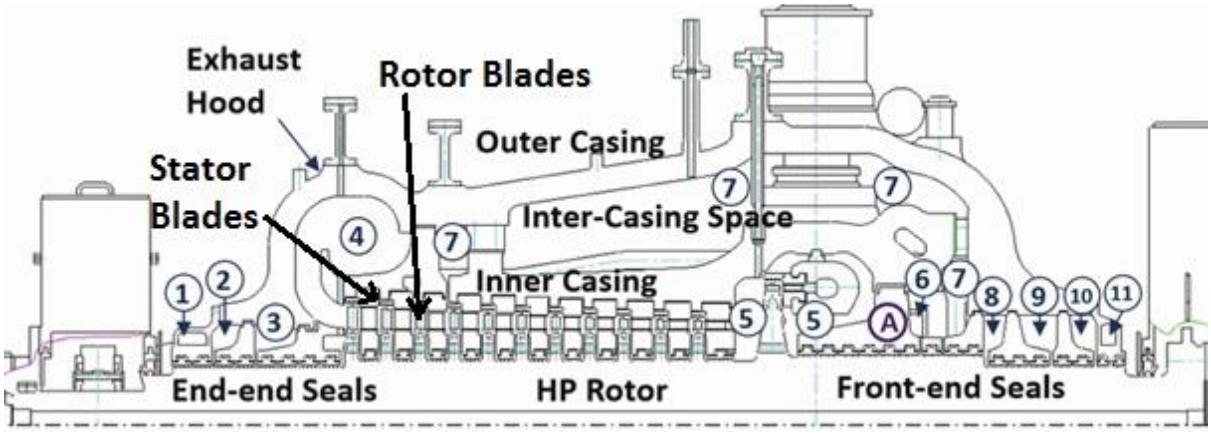

Figure 1. Cross-section of a steam turbine. [8]

Steam turbine can be single-staged or multi-staged. Nowadays are predominantly used multi-staged turbines. More stages enable to work with higher aggregate enthalpy difference, which is used to generate high powers. The capacity ranges from hundreds-of-kW to the 1900-MW. Steam turbines are primarily used in electric power generation for their capacity and efficiency. The most powerful steam turbines work with high-enthalpy steam, which increases the efficiency of the conversion. These are called ultra-supercritical (USC) pressure steam turbines. Inlet values of steam pressure extends from 24.1 to 31.0 MPa.g and from 593°C to 600°C for steam temperature. To give an image of such a turbine it is usually a three or more section machine. Typical arrangement of USC turbine starts with a single-flow high pressure (HP) turbine, followed by a single-flow or double-flow intermediate pressure (IP) section and one to three low pressure (LP) turbines with double flow. From inlet to outlet as steam's

energy is extracted, steam increases its volume up to multiple of 2000 of steam inlet. The expansion of the steam increases steam velocity. If the velocity of the steam is to stay constant, the cross-section area A has to grow larger, according to the continuity equation $\rho \cdot A \cdot c = Const.$ [16]

The extraction of steam energy leads to partial steam condensation, turning the steam into a wet steam. These drops of water damage the material, resulting in its erosion and possible corrosion.

3 Measuring chain at calibration

In order to stay competitive on the market, constant improvement in steam turbine efficiency, power-cost ratio, and delivery of the turbine performances based on customer's requirements is essential. The turbine is first designed via numerical models. The real turbine matches the designed parameters only as good as precise the numerical models and methods are. Results from experimental measurements of the already running turbines serve as a ground for development of even more precise numerical models. An approach for an experimental measurement is discussed on the following pages.

To ensure that the measured data are credible, a thorough calibration is essential. Calibration serves to investigate how the probe behaves during the measurement and in our case, gives us relation between the pitch angle and the measured pressures.

The probe to be successfully calibrated, a set of measuring equipment (measuring chain) and an experimental tunnel (simulates steam flow conditions) is required.

A 7-hole probe measures the pressures in the turbine, therefore the same probe is a subject of calibration. The probe is mounted onto a steel stem while measuring the pressures in the turbine. For the purpose of calibration, it suffices to manipulate with the probe head alone.

The probe is placed into a stand's probe holder. The stand's motors allow the probe holder to rotate the probe around its axis as well as in a horizontal plane. Yaw angle represents the rotational movement. Pitch angle represents the movement in horizontal plane. These angles can be seen in the fig. 6 . A computer software tailored for Doosan's needs controls the controller. Controller 1 is responsible for motor movements.

A Pitot-static probe measures simultaneously the static and total pressure and serves as a reference value. The Pitot-static probe is attached vertically to the same stand as the calibrated probe.

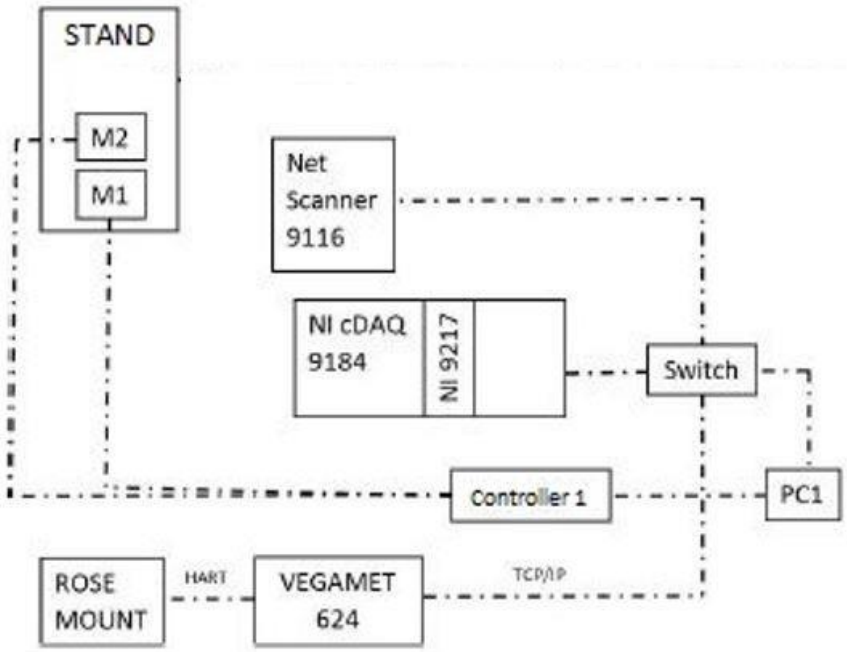

Figure 2. Key equipment of measuring chain.

The pressure transducer NETScanner 9116, manufactured by Pressure Systems, measures the seven pressures from the 7-hole probe and converts them into electrical signals. Switch processes the signals and forwards them to the computer to store the data. Pitot-static probe is also connected to the pressure transducer and similarly stores the data. Atmospheric pressure p_B is measured by an independent device ROSEMOUNT type 3051S. ROSEMOUNT communicates with VEGAMET over HART protocol. VEGAMET converts the pressure into digital signal. This signal is then sent to Ethernet network. VEGAMET uses TCP/IP protocol to communicate with the switch.

Figure 3. Pressure transmitter ROSEMOUNT [13] [left] and the probe stand [15] [right].

A resistant thermometer PT100 connected to NI 9217 card records temperature. The card measures resistance of a platinum wire. Inside the card is an A/C converter that converts the

resistance, voltage respectively into a digital signal. The card is plugged in NI cDAQ 9184 chassis. The chassis communicates with a PC over Ethernet network.

The data regarding pressures, temperature, and position of each measurement are stored in the computer. We use these data to produce calibration coefficients and calibration equations.

Calibration of the pressure probe requires an experimental wind tunnel. Doosan Škoda Power uses in-house wind tunnel to perform probe calibrations. Doosan's open-end low speed wind tunnel is about 15 m in length and has 2 m in diameter at the widest place. It is tapered on both sides, you can see it below. Circular exit area of 400 mm in diameter ends one side of the tunnel. On this end, a calibration of pressure probes takes place. On the second end of the tunnel is a source of compressed air sucked in from the space around. A ventilator ARK 800 from ZVVZ Milevsko and its 160 kW motor CAG HGIE2 315L1-2 are responsible for the necessary airflow. The motor's RPM is controlled through a frequency converter from ABB. It is important to know the velocity distribution at the tunnel exit and guarantee time stability of flow. The tunnel is designed in cooperation with scientists of Czech Academy of Science (AV ČR). The leader of my thesis, prof. Ing. Václav Uruba CSc., is one of them. [14] [15]

Figure 4. Experimental Tunnel. [15]

4 Measuring equipment at data acquisition

7-hole probe

The 7-hole probe can be used to measure pressures in two-phase environment, which is the case at the last-stages of the turbine. Its design was developed in cooperation of Doosan Škoda Power and SVÚSS Institute in Běchovice. The probe is attached to a steel stem through which impulse tubes are lined and lead to pressure transducer. Steel stem dimensions are 50 mm in diameter and 4.3 m in length. The length may vary according to need.

Figure 5. Pressure probe. [15]

Only the probe is subjected to calibration. The steel stem and the probe has to be taken apart, probe is then calibrated and then re-attached to the stem.

The 7-hole pressure probe records pressures at seven different places. Pressures p_1, p_2, p_3, p_4 describe the stream's incoming angle ε towards the probe. These holes are located vertically in the front of the probe. A pair of holes in the horizontal direction are pressures p_L and p_P. The probe rotates around angle α until pressure difference $\Delta p = p_L - p_P$ equals 0, thus the "zero angle measurement" condition is fulfilled. The last hole placed on the side of the probe is denoted p_B. [15]

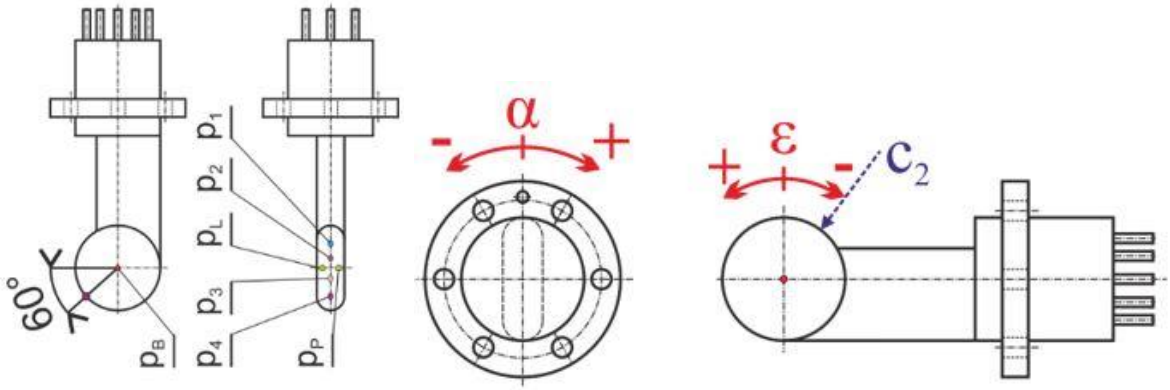

Figure 6. Denotation of probe's holes and angles. [14]

Pressure Transducer

Pressure transducer receives the information pressure information measured by the probe. Pressure transducer NetScanner 9116 is used and is suited for both an air and a steam measurement. The pressure is transferred via impulse tubes from the probe. The pressure is converted into numerical values in SI units that are further sent to a switch over TCP/IP to a PC. [15]

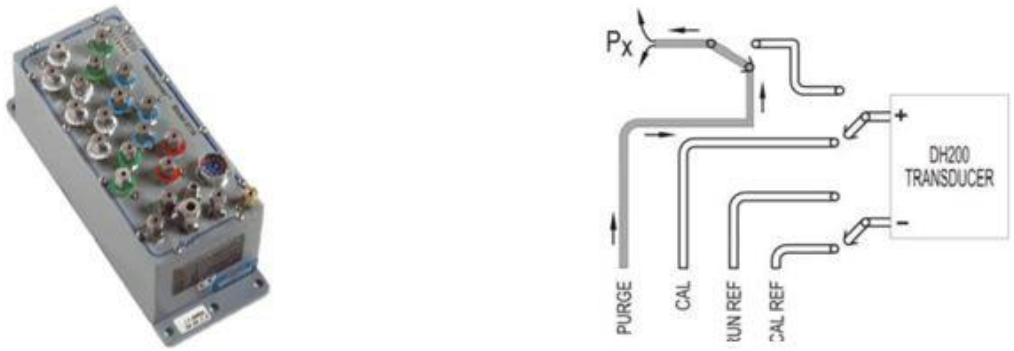

Figure 7. NetScanner 9116 and cleaning of impulse tubes. [15]

It is able to measure up to 16 pressure channels. The pressure transducer can clear the impulse tubes. This feature is possible due to a directional valve based on solenoid's operation within the machine. When the measurement takes place in wet steam, it is necessary to ensure that a condensate will not enter the transducer's channel. Hence, a water droplet separator is implemented into the routes. [15]

Water droplet separator

This device protects the channels of the pressure transducer against destruction caused by water droplets.

Figure 8. Design of customized water droplet separator. [15]

The device separates the impulse tube in two. Within the separator is inserted a separating net. The net hinders the water droplets to enter the upper impulse tube. It is not a regular part, Doosan Škoda Power put it together by itself. [15]

Continuous cleaning of impulse tubes

A variable area flowmeter is used to continuously clean the impulse lines. According to a graph, the air flow should not exceed 0.2 l/h. The flow rate is set based on error in measured pressure that is limited to 10 Pa. All the lines are influenced by the same error. The error is to be rectified prior to data evaluation. [15]

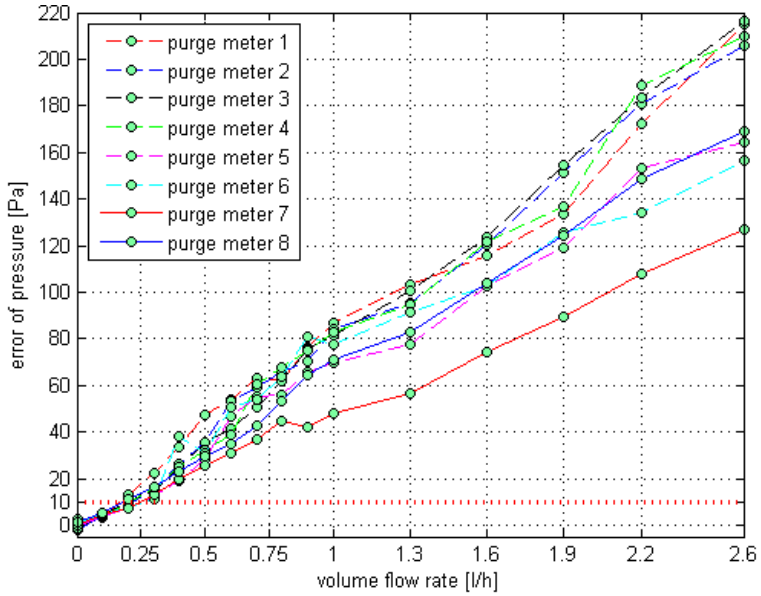

Figure 9. Relation of purging air flow rate and measurement error. [15]

During the data acquisition at the turbine, another more sophisticated equipment is used. It serves for measurement of absolute position of the probe. More specific, its radial position and its rotation. The steel stem is fixed to a place on the outer casing of the turbine, allowing only radial and rotational movement. [15]

Rangefinder and magnetic position encoder

A laser rangefinder LEICA DISTO is employed to measure radial distance of the probe from the fixed point of the turbine outer casing. The rangefinder uses interface RS232 that does not use WiFi or Bluetooth because it is forbidden in vicinity of turbine's generator. [15]

Figure 10. The rangefinder, the magnetic position encoder, the impulse counter. [15]

Second piece of equipment is the magnetic position encoder that encircles the steel stem. The position of the steel stem is determined through a number of points located around the circle. Each point records the radial distance between itself and the steel stem wall. Output signals are sent to an impulse counter, in our case IncRS232, which resends an altered signal using serial communication into the RS232 interface of the rangefinder. [15]

Serial Device Server

In order to transform the incoming serial signal from the rangefinder as well as the impulse encoder into Ethernet signal, a device called serial server is put in use. To be more specific, serial server EKI 1522 with 2 ports and capability to work with any incoming serial signal such as RS232, RS422 or RS485 was deployed, shown below. [15]

Figure 11. Serial Server. [15]

5 Calibration

In general, there are two approaches of data acquisition. In dependence on an approach, the appropriate calibration style is chosen.

If the probe is to be placed in one fixed position, the first approach, called non-nulling technique, is used. The data acquisition is simpler, however, the probe's calibration becomes more challenging. A calibration goal is to exactly define relations between angles α and ε and the measured pressures p_1 through p_4, p_B and static and dynamic pressure. The acquired data are then evaluated in the same ranges of angles α and ε as had been the case for calibration.

The static and dynamic pressures in the turbine are calculated based on regression equations stemming from the calibration. [14]

The second approach, so called nulling technique, requires more movement during the data acquisition, nevertheless, the calibration data processing is not as demanding as by the first approach. Probe is arranged in such position that pressure difference $\Delta p = p_P - p_L$ equals zero. Thereby the angle α is set. Probe may move in horizontal plane around angle ε. You can see a picture of the pitch and yaw angles here . During data acquisition in a turbine, the probe is unable to tilt to sides but can rotate around its axis. This means, the probe's pitch angle is fixed whereas angle α changes until the pressure difference condition is met. The probe adjusts angle α at each measuring point so the pressure difference condition is fulfilled. The static and dynamic pressures are calculated based on regression equations stemming from the calibration. [14]

The outputs of calibration are calibration curves, a system of regression equations. In our case, the nulling technique is utilized.

The same probe for data measurement in turbine is subjected to calibration. During the calibration, information about pressures, temperatures, time, angles α and ε are recorded. The sampling frequency and sample size can be arbitrarily chosen. In our case the frequency is 100 Hz.

Calibration curves

Calibration curves are given rise from calibration coefficients along the angle ε. The calibration coefficients are dependent of the measured pressures p_1, p_2, p_3, p_4 and p_B, see the formula (1).

$$k_{\varepsilon ij} = \frac{p_i - p_B}{p_j - p_B} \quad ; i = \{1,2,3,4\}, j = \{1,2,3,4\}, i \neq j \tag{1}$$

The following two formulas calculate the coefficient of dynamic and static pressure. Reference probe's static and dynamic pressures are put in use.

$$k_{D\,i} = \frac{p_i - p_B}{p_D} \quad ; i = \{1,2,3,4\} \tag{2}$$

$$k_{S_i} = \frac{p_i - p_S}{p_D} \quad ; i = \{1,2,3,4\} \tag{3}$$

Some of the curves may not be appropriate for further use. Things like sudden discontinuations or inflection points should be looked for. Areas around those problematic points are affected by higher uncertainty and for this reason are not recommended for further use. However, part of the curve can be used and it still yields valid results. Hence, an algorithm has to be implemented in order to successfully avoid the troublesome areas. A picture of suitable and partially suitable curves can be seen in fig. 12. [14]

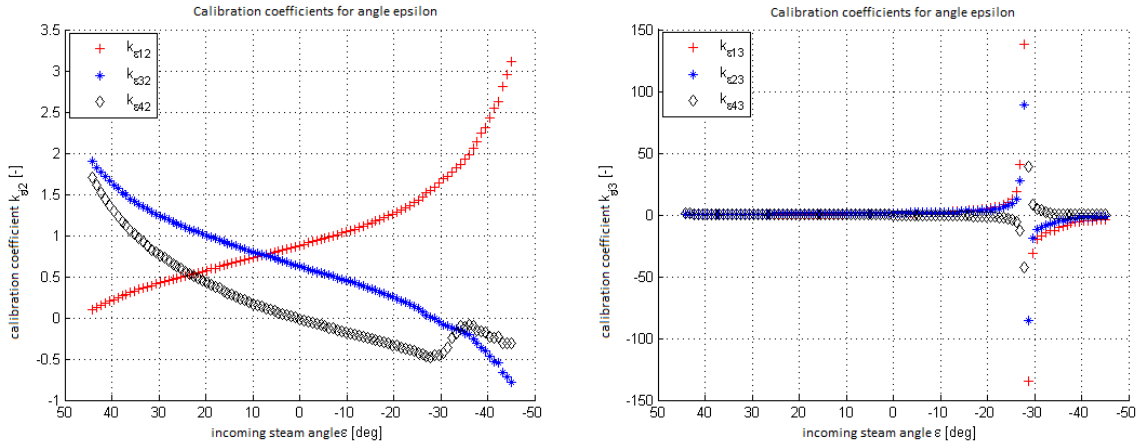

Figure 12. Different calibration coefficients. [14]

Regression equations

Regression equations, also called calibration equation, are polynomial functions that are fitted through the calibration data. We fit polynomial functions through suitable calibration coefficients.

The general form of a polynomial: $y(x) = b_{n+1} \cdot x^n + b_n \cdot x^{n-1} + \cdots + b_2 \cdot x + b_1$

The best fitting polynomials are further used for determination of the pressures and velocity components of the steam.

6 Calculation of pressures and velocity components

The calibration delivers the necessary polynomials. These polynomials are used for determination of the static and the dynamic pressure and velocity profile distribution along the blade of the turbine. [15]

$$p_D = \frac{p_i - p_B}{k_{D_i}} \quad ; i = \{1,2,3,4\} \tag{4}$$

$$p_S = p_i - \frac{k_S}{k_D} \cdot (p_i - p_B) \quad ; i = \{1,2,3,4\} \tag{5}$$

Total pressure equals to sum of static and dynamic pressure.

$$p_C = p_S + p_D \tag{6}$$

Steam density is used to calculate the steam velocity and is calculated from the static pressure and the quality of steam in IAPWS IF97 Matlab library.

$$\varrho = f(p_S, x); \quad IAPWS\ IF97 \tag{7}$$

Thermodynamic formula of steam velocity, shown below, is given by the local pressure conditions and type of medium.

$$c_2 = \sqrt{\frac{2 \cdot \kappa}{\kappa - 1} \cdot \frac{p_S}{\varrho} \cdot \left(\left(\frac{p_C}{p_S} \right)^{\frac{\kappa - 1}{\kappa}} - 1 \right)} \tag{8}$$

The spatial components of velocity can be determined through the measured angle α and the computed pitch angle. The trigonometric formulas (9), (10), (11) yield the velocity results in the radial r, tangential u, and axial z directions. [15]

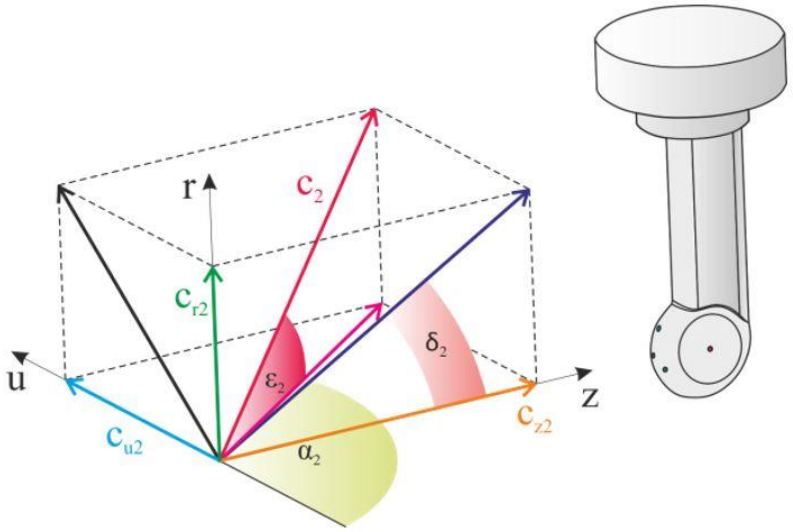

Figure 13. Velocity components. [15]

$$c_{r_2} = c_2 \cdot \sin(\varepsilon) \tag{9}$$

$$c_{u_2} = c_2 \cdot \cos(\varepsilon) \cdot \sin(\alpha - 90°) \tag{10}$$

$$c_{z_2} = c_2 \cdot \cos(\varepsilon) \cdot \cos(\alpha - 90°) \tag{11}$$

$$\delta_2 = \arctan \frac{c_{r_2}}{c_{z_2}} \tag{12}$$

7 Nulling of the probe

The acquisition of data from steam turbine is conducted at angle α where the pressure difference condition $\Delta p = p_L - p_P = 0$ is fulfilled. Angle α adjusts at each measuring point. The progress of curves of recorded pressure dependent on the turning angle α is portrayed below in the fig. 14.

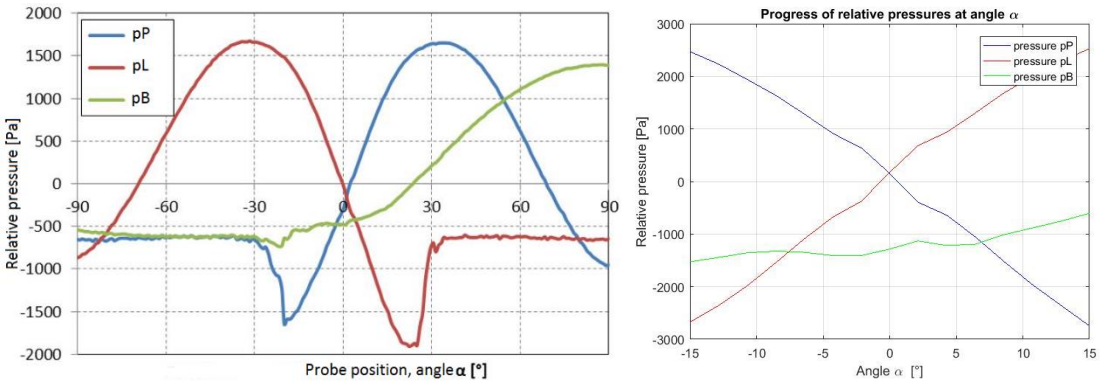

Figure 14. Pressure progress of p_L and p_P across a range of alpha, an illustrative picture [left] [15] and a real close-up [right].

On the left, there is a progress of three variable, ranging from -90° to 90° of a yaw angle. The close up on the right depicts only the crucial range of angle alpha. It ranges only within -15° and 15°. The pressure p_B is measured by the hole on the side of the probe. As the yaw angle changes, the pressures of p_L and p_P evolve. When one of them passes a separation point, the pressure progress rapidly changes. The pressure progress behind the separation point is not reliable and for this reason is not used to produce the regression equation. The areas of separations are easier to spot in the fig. 15 where the pressure difference is applied. It is easy to spot that the curve enters the areas behind the separation points at angle -19° and +19°. [15]

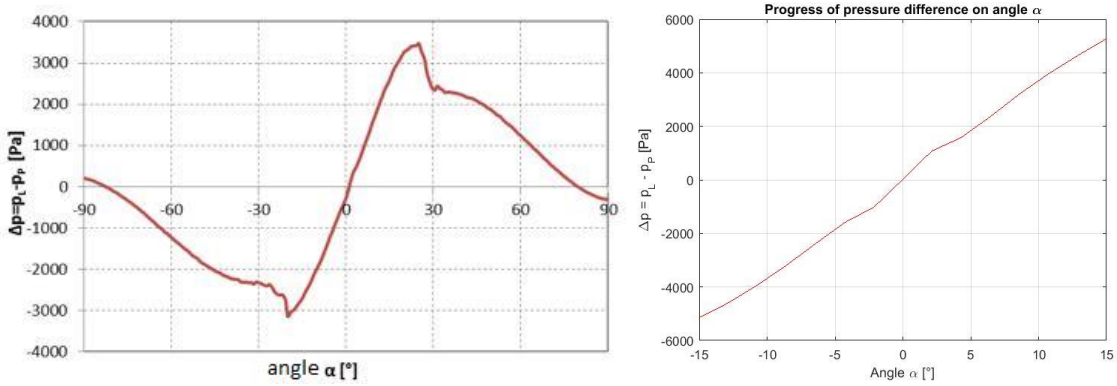

Figure 15. Pressure difference of p_L and p_P across a range of alpha. Illustrative picture [left] [15], close-up of real measurement [right].

The pressure difference is almost linear in the interval ⟨-19, 19⟩°. The close-up ranges only within -15° and 15°. This means there is an unambiguous dependency between the angle α and the pressure difference. This area is suitable for creation of regression equation.

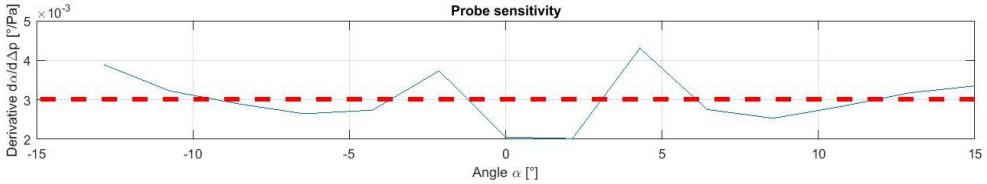

Figure 16. Progress of probe's sensitivity $\frac{d\alpha}{d\Delta p}$ and mean value in red.

Next two graphs describe the sensitivity of the probe and the uncertainty in correctness of the measured angle α. Within the interval, the mean value of sensitivity equals to 0.0030 °/Pa. The ability to measure correctly angle α is strongly dependent on the accuracy of pressure

measurement. If the pressure uncertainty takes up to ±33.3 Pa, then the uncertainty of the angle measurement reaches ±0.1 °. In reality the uncertainty is affected by more factors that the accuracy the pressure measurement. Nevertheless, from elaborations is confirmed that the uncertainty does not exceed ±0.5° for ±33.3 Pa pressure uncertainty. [15]

The regression function is depicted in the fig. 17.

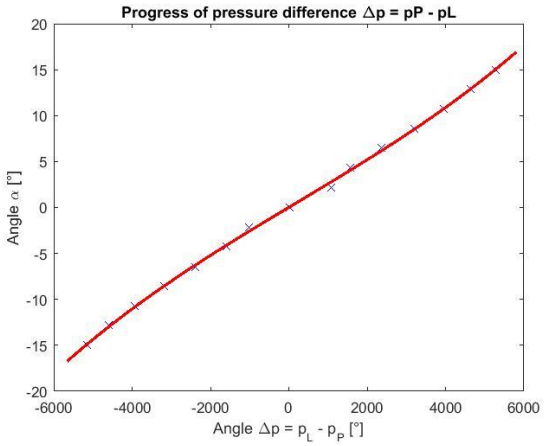

Figure 17. Regression function for Δp and ε.

The regression function describes only the pressure progress over the interval ⟨-15, 15⟩°.

The regression function is a polynomial of the third order that can be seen below.

$$y(p) = p_1 \cdot \Delta p^n + p_2 \cdot \Delta p^{n-1} + \cdots + p_n \cdot \Delta p + p_{n+1} \quad (13)$$

The coefficients for p_1 through p_4 can be seen in table 1.

Coefficient	p_1	p_2	p_3	p_4
Value	$1.159*10^{-11}$	$-6.000*10^{-9}$	$2.6*10^{-3}$	$1.33*10^{-2}$
n	3	2	1	0

Table 1. Coefficients of regression equation for angle α prediction.

These coefficients have to be set for each probe individually.

The regression equation works only for this limited interval, here ⟨-15, 15⟩°. Outside the interval, it yields misleading values.

When we land the probe outside of the interval described via the regression equation, we use a different method to move the probe into the desired interval. A new pressure difference $\Delta p = p_L - p_B$ comes in play. The probe cannot be positioned more than 75° away from the desired interval. We need to determine the orientation of rotation towards the ⟨-15, 15⟩° interval. A sign of the new pressure difference gives the orientation. If the difference is negative, the probe shall be rotated counterclockwise. If positive, then clockwise.

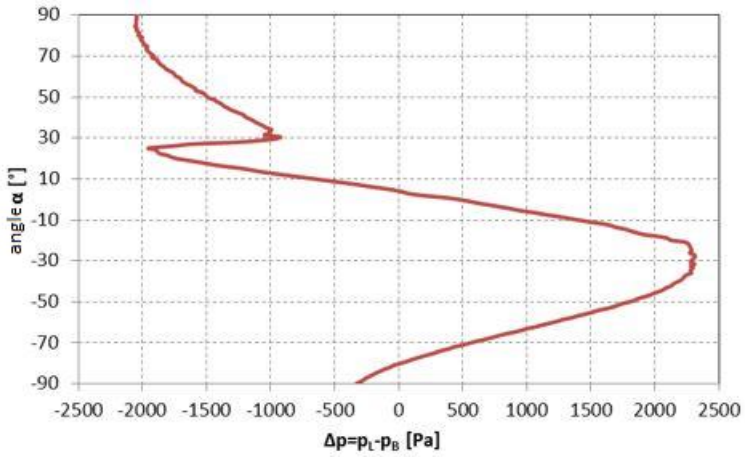

Figure 18. Orientation towards the desired interval. [15]

The process of probe "nulling" has to be done for each measuring point.

8 Compressibility of steam

When a calibration of a probe or a data acquisition takes place, it is necessary to consider the compression effect. With increasing Mach number, the compression effect grows. If not taken into account, the measured pressures deviate from the correct value. The significance of the deviation error directly correlates with the Mach number. This dependency for a Pitot-static probe is written in the formula (14) below. [15]

$$\epsilon_{stl} = \left| 1 - \left[\left(\frac{2}{\kappa \cdot Ma^2} \right) \cdot \left(\left(1 + \frac{\kappa - 1}{2} \cdot Ma^2 \right)^{\frac{\kappa}{\kappa - 1}} - 1 \right) \right]^{\frac{1}{2}} \right| \tag{14}$$

The calibration data are gathered at Mach number 0.2 which imposes less than 1% error in recorded pressures. The error based on Mach number is depicted in the figure below.

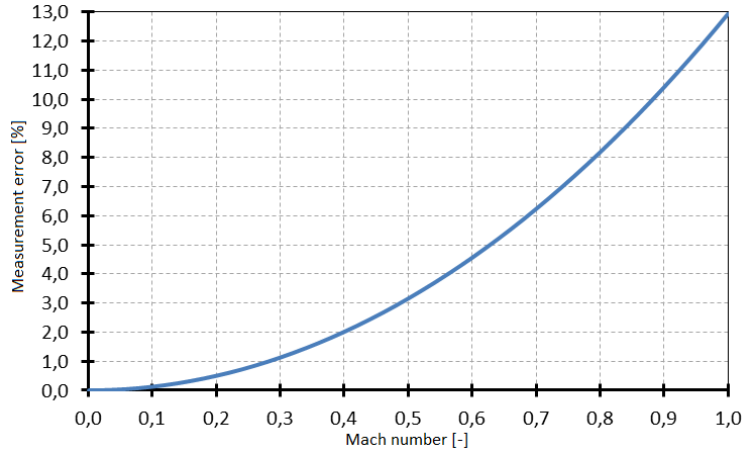

Figure 19. Measurement error based on Mach number. [15]

In order to tackle this error effectively, a calibration at higher Mach numbers is required. The calibration for 7-hole probe is done at VZLÚ (Czech Aerospace Research Centre). As Mach number becomes one of the parameters, calibration coefficients are no longer curves. They

become surfaces instead. The calibration coefficient is now a function of two variables, the Mach number and the pitch angle. Surface of calibration coefficient $k_{\varepsilon 32}$ is shown below. [15]

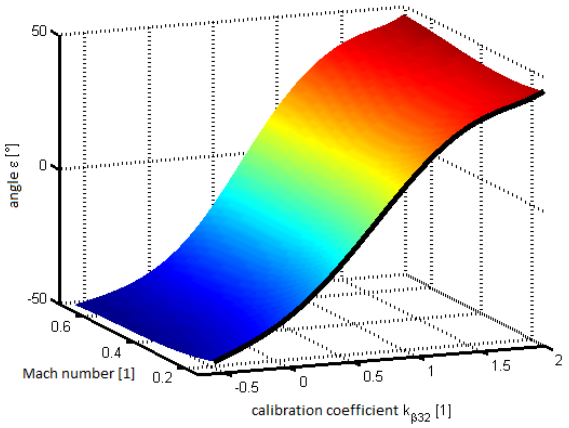

Figure 20. Calibration coefficient surface. [15]

Black curve in the picture is the calibration coefficient curve we are using throughout the thesis. Calibration of the probe for various high Mach number is not part of the thesis because the wind tunnel in Doosan's experimental facility is unable to reach high Mach numbers.

9 Data acquisition

Data acquisition from the turbine is not an easy task. The date of the measurement is set weeks sometimes months ahead. An intense communication between the power plant and Doosan Škoda Power is required. Other things such as authorization of turbine working conditions, passes to enable free movement in the power plant and the transport of the measuring equipment. The hardest part of data acquisition is to ensure flawless preparation and operability of the equipment. The exact order of turbine's working condition changes is determined prior to measurement and is done only once. A measuring team has only one chance to conduct the measurement properly. A quick but thorough check of the measured values and their saving is conducted. The team consists usually of at least 3 men. The transport of the necessary equipment, app. 750 kg, is physically demanding. Two men manage the measurement with the probe – data acquisition, step movements of the stand and data saving. The third person measures the static pressures and communicates with the control room of the power plant. [15]

The installation of the equipment has several steps. First, the sealing ring is installed, followed by firm attachment of the probe stand and connection to the measuring chain described in chapter 3. The probe is inserted into the turbine while running under supervision of a chief power plant operator. Changes in turbine's working conditions can lead to change of other parameters and there is no way to correct these changes. One of the common changing parameter is the vacuum level in LP sections. Generally, the grid itself gives the rpms and a regulator sets a power output, the other parameters are adjusted accordingly. [15]

Figure 21. Overview of the probe stuck through the outer casing reaching the bottom of a blade [left]. Transducer and water droplet separators set at the top of a rack [right]. [15]

In the fig. 21 on the left, you can see the stand placed on top of the sealing ring that is attached to the outer casing of the LP turbine section. Through both is passed the probe that is moved via the massive hand-operated stand. On the right side, the rack holds the pressure transducer, variable area flowmeters, water droplet separators and impulse tubes.

After the successful measurement, we move towards the second stage, which is data processing. Data processing and interpretation partially takes places during the acquisition phase via a custom-made measuring application. A crew team member can easily evaluate the trustworthiness of the acquiring data. If their values do not match expected values, it points at a fault in measuring chain, equipment or turbine regulations. Larger and more thorough part of data processing takes place back in the office. The large data are processed with help of Matlab software. [15]

9.1 Custom-made measuring application

The application serves as a tool to set up all equipment settings and communication within the measuring chain, data acquisition, writing, saving and assessment of the primary data. All variables are being continuously saved to the application and their progress is immediately interpreted on the user interface. The staff of the measuring team glances over the recorded pressure and velocity progress to check whether the recorded data correspond to their expectations. This is an essential part of the measurement because if overlooked the acquired data might or might not be correct and the whole measurement might be vain. If the data seems to comply with the expectations, it is proceeded to acquisition of the whole data set. [15] [2]

The application was developed in co-operation with Department of Cybernetics of Faculty of Applied Science. It was developed in software LabVIEW 2003. It uses the measured variables as an input for online calculations of steam parameters. These calculations happen in the background of the software and are interpreted in the front window. Three tabs are located at the bottom of the user-friendly front window. [2]

The first tab serves for basic setting of the equipment of the measuring chain, setting of the desired sample format and first overview of the data. In the textboxes highlighted in blue on

the left hand side of the screen is set the direct connection between the software and the measuring chain components. The hardware setting can be changed or kept as pre-set. A prompt window pops up at the software start and lets us choose. Right next to it, highlighted in green, one can see the active and inactive channels of the pressure transducer and the measured pressures. If the channel box is not ticked, data will be nor measured nor saved. Pass by to the right, there is several blue colored textboxes where sampling frequency and number of samples is set. The right half of the screen shows bar diagrams depicting the pressure for each hole of the probe and prediction of probe nulling angle α. [15] [2]

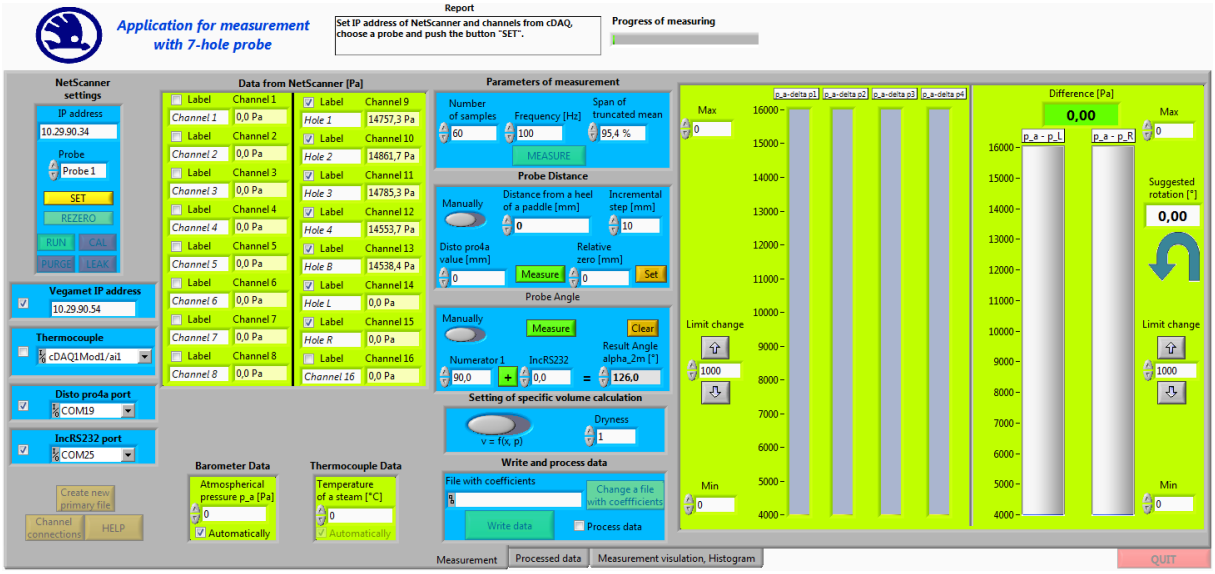

Figure 22. First tab – Measuring chain settings and basic pressure overview [15]

The second tab is used for data management. It allows the user to amend the data by their deletion, transfer, addition, or saving. The screen on the right side of the tab displays the progression of the yaw angle along the blade length. [15] [2]

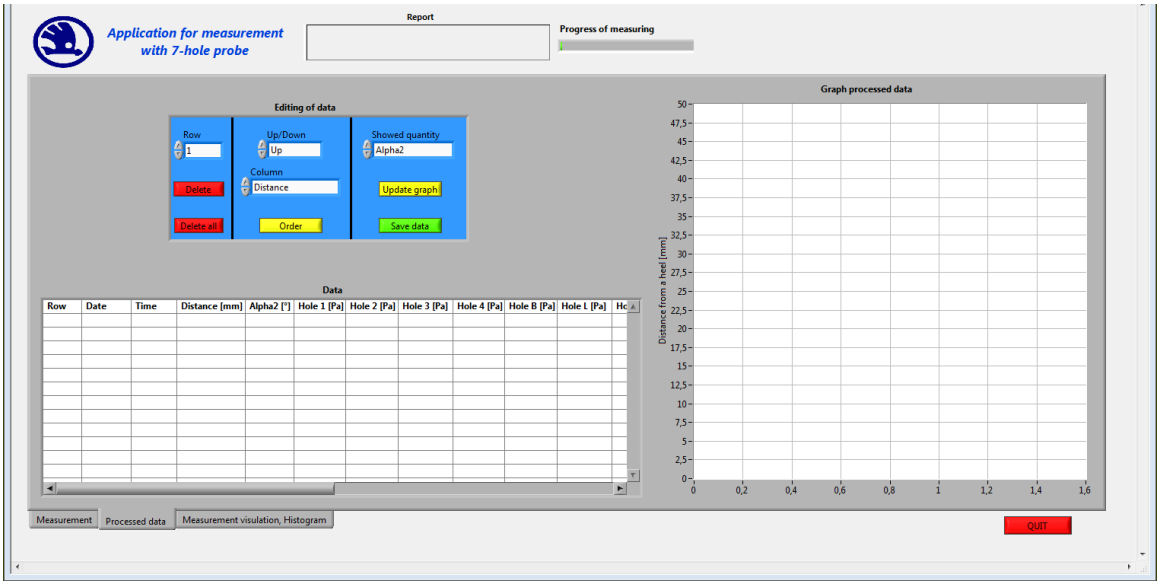

Figure 23. Tab with data management and their interpretation. [15]

On the last tab, there are two empty windows. Although they are empty at first, user can pick any channel to show. The white window graphs the variable progression over time whereby

the yellow window depicts data distribution. Two or more variables can be selected at the same time to display their progress over time. [15] [2]

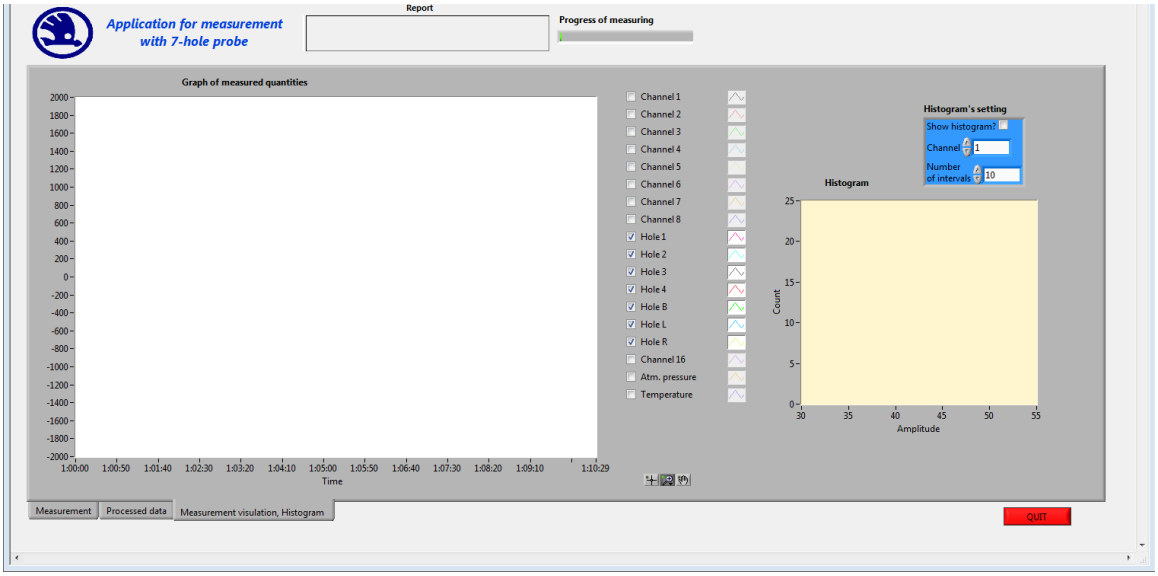

Figure 24. Visualization of measured data and their distribution. [15]

9.2 Measurement of steam wetness

Water is the medium of a secondary circuit of any power plant working with a steam turbine. Water properties change as the water changes its state from saturated liquid to saturated steam.

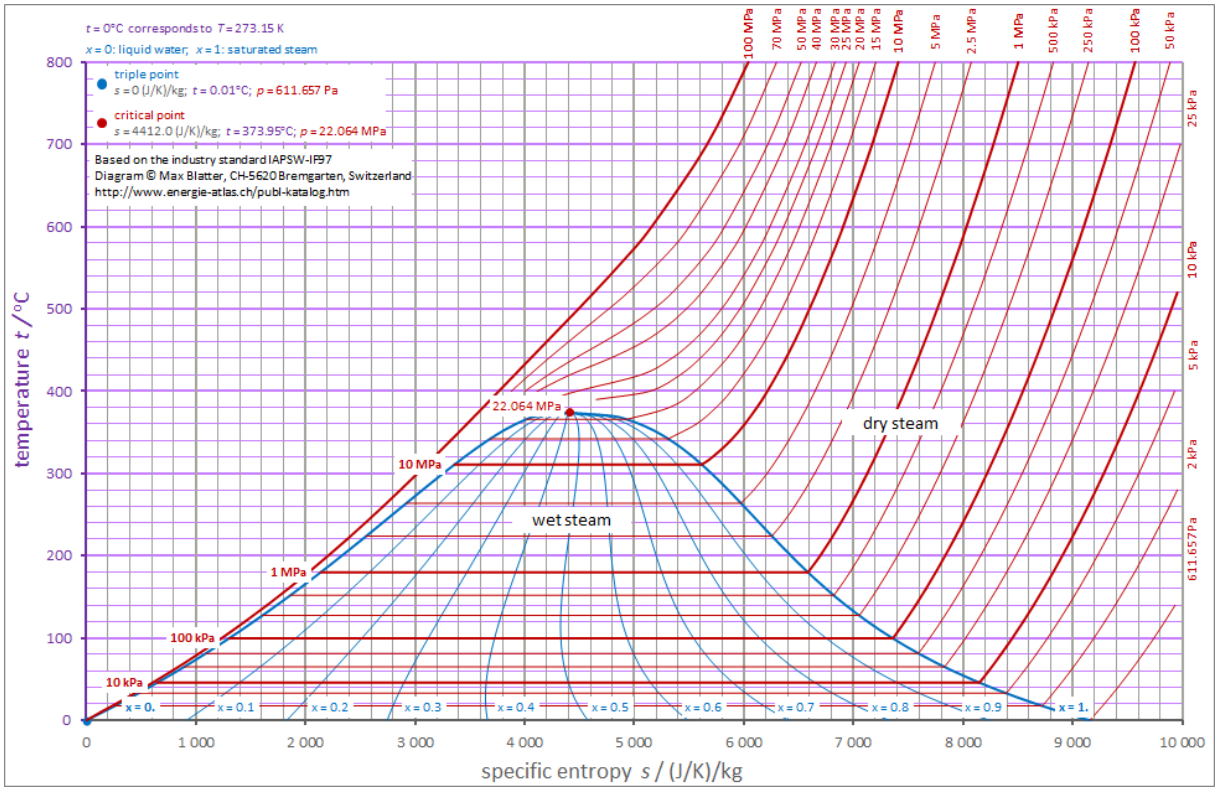

Figure 25. T-s diagram of steam [19]

Determination of properties for single phase is simple. All you need is temperature and pressure. However, wet steam is not a single phased medium any more. Quantity called wetness describes the proportion of water to the mixture of steam and water. Wetness equals "1 – dryness". Dryness calculation is given by formulas (15) - (17).

$$x = \frac{v - v'}{v'' - v'} \tag{15}$$

in which *v* is a specific volume of wet steam

$$x = \frac{h - h'}{h'' - h'} \tag{16}$$

in which *h* is a specific enthalpy of wet steam

$$x = \frac{s - s'}{s'' - s'} \tag{17}$$

in which *s* is a specific entropy of wet steam

Where superscript ' denotes the saturated liquid line and superscript '' the saturated vapor line. Which are visible in the fig. 25.

In the two-phased region, all properties such as volume *v*, enthalpy *h*, internal energy *u*, entropy *s*, speed of sound *w* can be calculated by steam tables IAPWS IF-97, where at least one of the input parameters has to be the dryness.

The dryness is indirectly calculated from measured water content in the steam by a spectrometric probe. The probe is attached to the end of a steel stem. The stem is inserted into the turbine outer casing at the same spot as is the case for pressure probe. Then we have it moved along the blade length. Some probes have longer heads than others do, which prevents us from taking measurement at the root of the blade. The probe design with head type V-2 is portrayed in the figure below. [9]

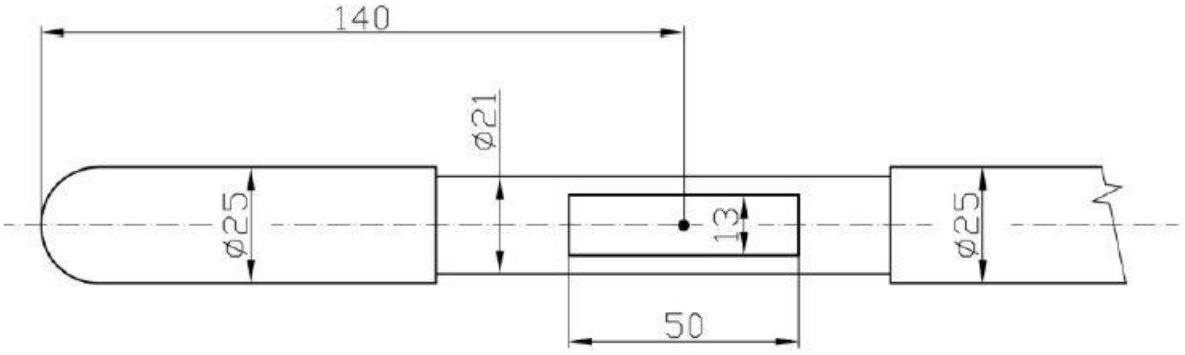

Figure 26. Dimensions of spectrometric probe V-2. [9]

In the cylindrical body of diameter of 21 mm is milled a rectangular hole. The rectangular hole has dimensions L x 13 mm, where L equals 50 mm. Wet steam at the last stages of the turbine blades passes through this hole. In axial direction of the probe, is a ray emitter and ray absorber. The water droplets cause distortion of the receiving signal. Due to the light ray dispersion, the receiving intensity will decrease. The decrease correlates with the density of

water droplets. Signals are tested before the steam passes through the sensor and then while the turbine runs. After each measurement, we compare the two received ray intensities. Different wavelengths λ within 200 and 1000 nm range are tested. [9]

Let us get into a little more detail about the light generation and absorption. Kolovratník used for the wetness measurement a spectrometric method. This spectrometric chain consists of a halogen-deuterium source attached to the stem on the outside, a light guide that leads the light towards the emitting collimator. Then the light with intensity I_0 passes through the layer of air or steam thick L mm. A collecting collimator gathers the light with intensity of I and leads it through another light guide towards an external spectrophotometer. Both collimators are snuggly fitted over the cylindrical parts with diameter 25 mm. The spectrophotometer creates a digitalized signal of intensity for each wavelength. [3]

The measurement in wet steam has two steps. First is to measure the received beam intensity when no steam passes by. This intensity is called a referential intensity and is denoted I_0. Second measurement is conducted when steam passes through the probe and the light beam is distorted and therefore the received intensity is lower. This intensity is denoted I. Several wavelengths λ from the range 200 – 1000 nm are selected and both steps are done individually for each. Several wavelengths are chosen to ensure a proper determination of water droplets scatter φ(D) and their sizes D. [9]

Water droplet scatter φ(D) is calculated from a system of equations, so called system of Fredholm integrational equations of first order. The general form of the equation reads

$$\frac{1}{L}\ln\left(\frac{I_0}{I}\right)_i = \frac{\pi}{4}N_v\int_0^{D_\infty} Q\left(\frac{\pi D}{\lambda_i}\right)\cdot\varphi(D)\cdot D^2 dD \tag{18}$$

Where $\left(\frac{I_0}{I}\right)$ is a ratio of initial beam intensity and received beam intensity, N_v is a number of elements in unit volume, $Q\left(\frac{\pi D}{\lambda}\right)$ is a coefficient of light scatter according to Mie theory, D is a diameter of a particle, wavelength λ. [9]

However, this method has a drawback. Results of the Fredholm system of integrational equations are susceptible to even small deviations in intensities and their ratio $\left(\frac{I_0}{I}\right)$ respectively. [9]

Different approach, a numerical method, to calculate the water droplets scatter φ(D) is developed by Academy of Power Energy FS ČVUT in Prague. This RNL method is appropriate for evaluation of integral polydispersion characteristics. [9]

One of the polydispersional characteristics is the steam wetness y. [9]

The steam wetness formula reads

$$y = \frac{I}{1+I}\ where\ I = \frac{\pi}{6}\frac{\rho_k}{\rho_p}N_v\int_{D_{min}}^{D_{max}}\varphi(D)D^3 dD \tag{19}$$

ρ_k density of liquid portion (water), ρ_p density of gas portion (steam)

Wetness is corrected based on CFD model that considers density change of the medium near the probe. The change in density influences the volume concentration of elements N_v. [9]

10 Speed of sound

The proper determination of the speed of sound in the two-phase region is done via Matlab library IAPWS IF97. This library compiles the whole knowledge of calculation of thermodynamic properties. The name IAPWS stands for International Association for the Properties of Water and Steam. Steam tables are converted into the modern form to enable engineers to use computers for fast and easy determination of values. The steam tables are based on ASME standard, which is an American published document. The number 97 denotes the year when these steam tables were approved to replace the old IFC-67 formulation. [7]

IAPWS IF97 allows the user to calculate any thermodynamic property within the two-phase region based on at least two known properties, which at least one of them should be pressure or temperature and the other quality of steam. [7]

It has turned out that the library does not hold true for the calculated speed of sound when the steam quality is higher than 95 %. [15] The steam tables IAPWS IF-97 do not work effectively. It is because a qualitative aspect of the water droplet distribution and size is missing. We are not able to tell just from the quality of steam and be it a pressure or temperature of the steam, how diverse the environment of the wet steam is that the sound comes through. [15]

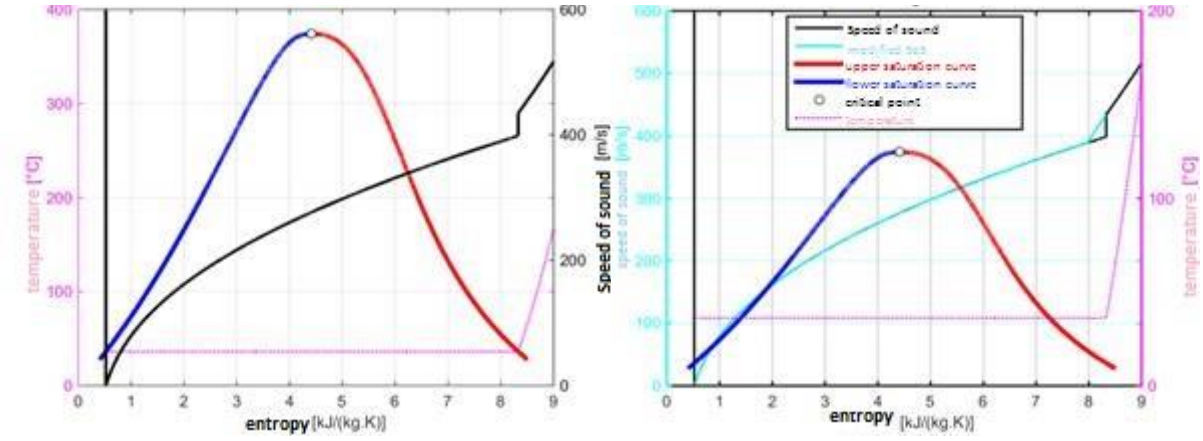

Figure 27. Standard IAPWS IF-97 speed of sound [left] and modified speed of sound [right]. [15]

Whereas the steam tables IAPWS IF-97 assumes thermodynamic condition of steam equilibrium and the speed of sound is calculated by Newton-Laplace equation (in black). Nevertheless, the assumption does not hold true when the expansion speed is high. At the high expansion speeds, thermodynamic condition of steam is not in equilibrium anymore and it is characterized by exchanges of energy, momentum and mass between the two phases. Those processes influence the speed of sound. As a rule of thumb, we can say if the steam quality ranges from 94.5 to 100 %, the difference between the true speed of sound and speed of sounds calculated under the thermodynamic equilibrium condition is the highest, up to 10 %. [15] [9]

Both of the approaches are missing the qualitative aspect of the wet steam and therefore the values of the speed of sound may widely vary based on used approach.

11 Uncertainty of measurement

Uncertainty of measurement is a qualitative property. It is a doubt of a result of any measurement. The doubt tells us how trustworthy the measurement is. Every device suffers from a margin of doubt. Therefore, we express the result as an interval where the true value is, with certain confidence, located.

The doubt is a consequence of mistakes happing during the measurement. There are two main uncertainties, type A and type B. [14]

The sources of uncertainty and error

Uncertainty does not concern only the measured variables but also many that are not measured. Those that directly or indirectly influence the measured variables. It would be very laborious and financially demanding to measure every single variable that has an effect on accuracy of the measurement. It is important to select correctly only the most influential variables. These are then recorded and used for determination of the true values. Some of the most common uncertainties are given here:

• The measuring instrument can suffer from errors due to wear, aging, poor readability, noise (for electrical devices)

• The instable nature of the measured item/variable

• The measurement process, its feasibility and suitability

• "Imported" uncertainties due to instrument calibration (if not calibrated, the uncertainty would be much worse and also unknown)

• Operator skill to meticulously set up the measurement or read-off values

• Sampling issues that do not satisfactorily represent the process

• Effects of environment on the measuring instrument or the measured item. [1]

If we knew the specific uncertainties for each, we might compensate for them. Nevertheless, we do not usually know how their uncertainties affect other variables and their uncertainties; therefore, we say they contribute to the overall uncertainty in the measurement. [1]

Uncertainty can be expressed in absolute or relative terms. The absolute term means that the measured variable is expressed in form of an interval:

$$y_m = y_s \pm y$$

Where y_m is the measured value, y_s is the median value, and y is the uncertainty. [14]

The uncertainty has to be of the units of the measured variable.

The relative term is expressed as percentage of the median value. The relative uncertainty δy is calculated as follows

$$\delta y = 100 \cdot \frac{\pm y}{y_s} = 100 \cdot \frac{y_m - y_s}{y_s}$$

Expressing the uncertainty in relative terms is favorable because it makes it easier to compare accuracies of different measurements. [14]

General kinds of uncertainty

The uncertainty can be of a random nature or systematic.

Random – contain all the phenomena that we cannot influence or cannot measure even though they still affect the result of the measurement. It is when the repeating measurement of the same quantity yields a randomly different result each time. Statistical analysis is conducted to estimate what the true value might be and what data are still highly probable to occur. [1]

Systematic – those uncertainties are constant at similar conditions and repeated measurements. It is sometimes hard to tell that they are even there. They are the consequence of the used method or instrument. Instrument specification usually shares the value of systematic uncertainty. It can be for example non-linearity, shift of null value or thermal sensitivity. This uncertainty can be limited through calibration of the measuring device or change of the measuring method. [1]

Uncertainty vs Error

Uncertainty and error are not interchangeable expressions. Whereas the uncertainty is a qualitative property that tells us how trustworthy the results are, the error is a quantitative property, giving us a numerical value, how much the measured and assumed true value differs.

"Error is the difference between the measured value and the 'true value' of the thing being measured." [1]

"Uncertainty is a quantification of the doubt about the measurement result." [1]

Every known error we try to minimize or eliminate. Then, however, raises the question whether the complete elimination was successful and how to prove the measurement does not carry residual error? This is when margin of doubt comes to play.

To make good and truthful measurements, it is necessary to work with devices that have their measuring uncertainties proven and tested. This can be used for different occasions such as:

Calibration – requires certificate to ensure certain measurement uncertainty

Test – decides whether the device can conduct certain task, pass or fail result

Tolerances – to decide whether the tolerance of a product is met when taking the uncertainty in consideration. [1]

Distribution of errors

The distribution of a given set of data can have various forms. The most common one is the normal distribution and we are going to discuss it here. Other distributions can be the uniform distribution or triangular or M-shape (two-peaked) or skewed (lop-sided).

Normal distribution, also called Gaussian distribution, shows that set of data are more likely to fall near the average rather than further away.

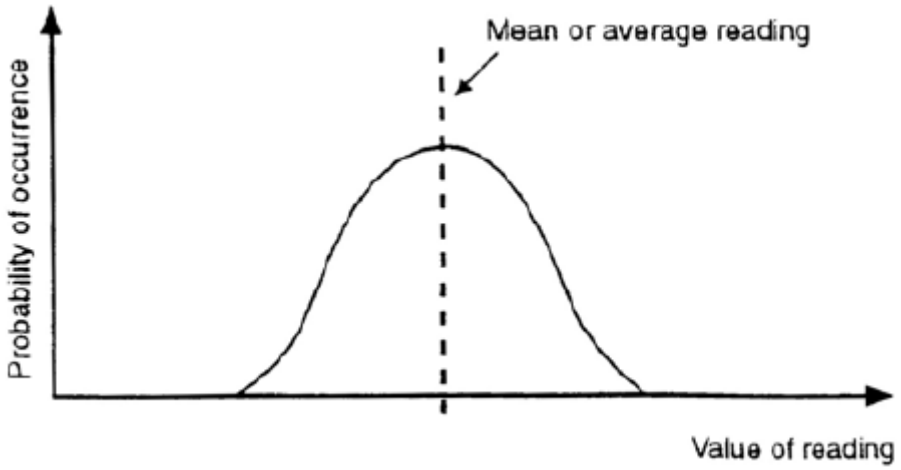

Figure 28. Sketch of a Gaussian distribution. [1]

Calculation of Uncertainty

First, we need to understand what the sources of uncertainty are. Second, we have to estimate the uncertainty size for each source individually. Lastly, we combine all those individual uncertainties to derive the overall uncertainty. Combinations of these uncertainties follow clear rules based on their type.

Regardless of the sources of the uncertainties, two approaches exist to estimate them, 'Type A' and 'Type B' evaluations. Usually both of them are present at each source.

Type A evaluations: "uncertainty estimates using statistics (usually from repeated readings)" [1]

Type B evaluations: "uncertainty estimates from any other information. This could be information from past experience of the measurements, from calibration certificates, manufacturer's specifications, from calculations, from published information, and from common sense" [1] They are uncontrolled, unmeasured resp. factors and their mean values are equal to zero. They are considered to have constant mean value and constant standard deviation (STD). Their mean values are described as systematic error/uncertainty and their STD is a contribution to the STD of the measured variables. [14]

Although one might incline to the opinion that 'Type A' is the 'random' kind of uncertainty and 'Type B' the 'systematic' kind of uncertainty, it is not necessarily true.

When we combine those uncertainties, it is necessary they have the same units and same level of confidence. What you can do is to standardize the uncertainty. A standard uncertainty has a margin that corresponds to one standard deviation.

Calculation of standard uncertainty for a Type A evaluation

The uncertainty is dependent on the number of readings within the set. The greater the number, the lower the uncertainty. Historically, this standard uncertainty is called the standard deviation of the mean. The calculation reads:

$$u_A = \frac{s}{\sqrt{n}} \tag{20}$$

Where u_A is the standard uncertainty, s is the estimated standard deviation of the set and n is the number of readings in the set. [1]

Calculation of standard uncertainty for a Type B evaluation

When the data are more scarce, sometimes the most we might get from it are the upper and lower limits of uncertainty. With a use of histogram, we might assume what the distribution from a given set of data are. Each distribution has different value for k. The normal distribution has k = 2, uniform distribution has k = $\sqrt{3}$ and triangular has k = $\sqrt{6}$. The standard uncertainty calculation reads:

$$u_B = \frac{a}{k} \tag{21}$$

Where u_B is the standard uncertainty of Type B, a is the half-width of the upper and lower limit of the distribution and distribution coefficient k. [1]

Other type B uncertainties and their limits can be given by previous measurements, uncertainty of device from OEM or calibration certificates. [1]

Combining standard uncertainties

The individual standard uncertainties can be combined by summation in quadrate, or also known as 'root sum of the squares'. The simplest way to combine the uncertainties is by addition or subtraction of the individual standard uncertainties. It interprets the final effect of uncertainties of type A and type B on the same variable. Formula for the combined uncertainty:

$$u_C = \sqrt{\sum u_{A_i}^2 + \sum u_{B_i}^2} \tag{22}$$

Where u_C is the combined standard uncertainty, u_A is the standard uncertainty of type A and u_B is the standard uncertainty of type B. [1] [16]

Coverage factor C

The standard uncertainty gives its value for one standard deviation. To scale the uncertainty and adjust the level of confidence, a cover factor comes in play. It changes the range of the uncertainty. Multiplying the combined standard uncertainty by a coverage factor gives a result, which is called the expanded uncertainty U.

The formula for it is written below:

$$U = C \cdot u_C \tag{23}$$

The value of coverage factor is selected based on the dataset distribution and the desired confidence level.

Coverage factor yields those values for a normal distribution

C = 1	for a confidence level of approximately 68 %
C = 2	for a CL of app. 95 %
C = 2.58	for a CL of about 99 %
C = 3	for a CL of about 99.7 %

Other distributions have different coverage factors.

Conversely, you can derive the standard uncertainty when the expanded uncertainty and coverage factor is quoted. This is often the case for an uncertainty noted in calibration certificates. To do so, divide the expanded uncertainty by the coverage factor. [1]

12 Statistics

Statistical analysis of data give us the notion what data set we are dealing with. For purpose of this thesis, we are going to use exploratory analysis of one-dimensional data. Graphical methods of exploratory data analysis are used for complex evaluation of statistical peculiarities of data. The primary data are used for further purposes; hence, a check of the fundamental parameters is necessary. These parameters can be presented as trends in data, data's skewness and kurtosis, variance, standard deviation, local data concentration, etc. We have the measured data compared with theoretical (normal) distribution. [16] [12]

Trend and periodicity
Omitting check for trends and periodicities of the data can lead to some significant problems down the road. Data set with presence of trends does not comply with the normality condition. The repercussion of not having a normal distribution is that common analysis tools cannot be used. Therefore, a check of repetitive changes in trend directions is necessary. Trends and periodicity can be investigated using various tools, such as periodograms or less time-consuming Fisher or Siegel tests. Periodiogram is more suitable for data that we suspect or expect to have harmonic components. We evaluate the peaks of amplitudes at each harmonic component. Fisher and Siegel tests test compliance of data to their hypotheses. [16]

Location and scale parameters
Mean, median and mode give us the location parameter of the data distribution. They are a part of the fundamental task of any statistical analysis. They are to give a typical value that best describes the data. There are three definitions of the location parameter. All answer the questions of typical value in slightly different, but still correct, manner. [4]

Mean, also referred to as the average of the data set, is equal to sum of the data points divided by the number of data points.

$$\bar{x} = \sum_{i=1}^{N} \frac{x_i}{N} \tag{24}$$

Median value from the data set where half of the data values are below this value and half above. Graphically it is the middle value of an ascending or descending order of the data set. [4]

$$\bar{x} = x_{\left(\frac{N+1}{2}\right)} \; if \; N \; is \; odd \tag{25}$$

$$\bar{x} = \frac{x_{\left(\frac{N}{2}\right)} + x_{\left(\frac{N}{2}-1\right)}}{2} \; if \; N \; is \; even \tag{26}$$

Mode is the most frequently occurring value from the dataset. It is easy to see in histogram. Mode is the midpoint of the highest peak. [4]

In normal distribution fall mean, median and mode together. This is, however, not the case for any other distribution or even slight deviation from normal distribution. [4]

The more mean and median differ, the more it points out at nonnormality of the data. The difference between the mean and the median can be expressed as absolute difference between the two values or in relative difference to the mean.

$$Diff_{abs} = |Mean - Median| \tag{27}$$

$$Diff_{rel} = \frac{|Mean - Median|}{Mean} \tag{28}$$

Extreme tail values or outliers less affect some other location parameters. For example, Min-Mean computes mean within the 25th and 75th percentile or Trimmed Mean that calculates mean from all data except the 5 % points in both tails. [4]

It is common to know the variability of the data. How much are the data spread about the mean and in the tails. Various methods to calculated spread will be introduced. Some are affected less by the tail values and some more. [5]

Histogram is an effective graphical technique for showing both components of the spread.

Variance gives us approximately the average squared value of distance from the mean. This method is highly affected by the tail values. It is because the distance from mean is the greatest and additionally squared. [5]

$$s^2 = \sum_{i=1}^{N} \frac{(x_i - \bar{x})^2}{N-1} \tag{29}$$

Where $\bar{x}$ is the mean of the data, N is the number of elements in the data set.

Standard deviation is the square root of the variance. The units of spread again match the original data, which is not the case for variance. [5]

$$s = \sqrt{\sum_{i=1}^{N} \frac{(x_i - \bar{x})^2}{N-1}} \tag{30}$$

Range is defined as the distance between the largest and smallest data set value. This spread is only given by two extreme values; hence, it does not represent the spread near the center of the data. [5]

More methods exist and they are more or less affected by the tail values, which influences the results of estimate of the variability of the data. For example, average absolute deviation is less affected by the extremes in tails. The same applies for median absolute deviation and interquartile range. Interquartile range yields a better representation of the data close to the mean. [5]

Skewness and kurtosis

When the data distribution does not match the bell curve, it is because the data are skewed. Mean, median and mode no longer fall together. The definition of skewness in Engineering Statistics Handbook reads "Skewness is a measure of symmetry, or more precisely, the lack of symmetry. A distribution, or data set, is symmetric if it looks the same to the left and right of the center point." [6]

When the data distribution is skewed to the right, the data have a long tail that extends to the right. This is also called the positive skew. When skewed to the left, the left side of the data extends farther. Which we call the negative skew. [17]

Mean, median and mode in positive skewed data set [17]

- Mean is always greater than the mode
- Median is always greater than the mode
- Mean is most of the time greater than median

Mean, median and mode in negative skewed data set [17]

- Mean is always less than the mode
- Median is always less than the mode
- Mean is most of the time less than median

Calculation of Pearson's first coefficient of skewness gives an explanation why the data skewed to the right has positive skewness. Pearson calculates the coefficient as a subtraction the mean from the mode ("mean" – "mode") and the difference is then divided by the standard deviation. The difference divided by standard deviation gives us dimensionless number. The result greater than zero because the 'mean – mode' difference is positive. [6]

Data skewed to the left has a negative result of Pearson's first coefficient because the mean is always less than the mode.

The Pearson's first coefficient is considered to be an easier formula to give a general overview. The common calculation takes into account all the data values provided. Down below is given the Fisher-Pearson coefficient of skewness formula:

$$\widehat{g_1} = \frac{\sum_{i=1}^{N} \frac{(x_i - \bar{x})^3}{N}}{s^3} \tag{31}$$

Many software programs calculate the skewness from adjusted formula for Fisher-Pearson coefficient of skewness. $\widehat{g_1}$ is multiplied by a coefficient that adjusts the skewness in wide ranges of samplings. Smaller sampling numbers are multiplied by a greater number and for large sampling numbers the coefficient approaches 1. It gives a more precise skewness result. [6]

$$\widehat{G_1} = \frac{\sqrt{N(N-1)}}{N-2} \cdot \frac{\sum_{i=1}^{N} \frac{(x_i - \bar{x})^3}{N}}{s^3} \tag{32}$$

Where N is the number of samples, x is the value of data i, $\bar{x}$ is the mean, and s is the standard deviation.

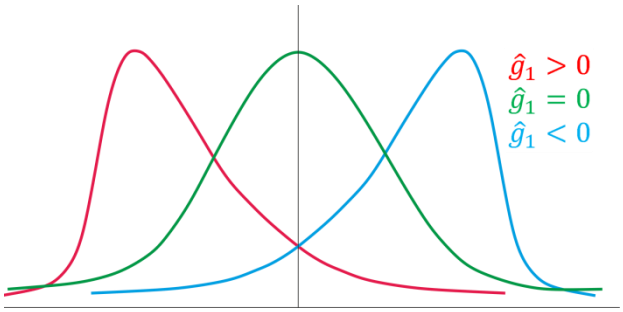

Figure 29. Data distributions and their skewness coefficient values from Fisher-Pearson. [16]

$\widehat{g_1} > 0$: Positive skewness
$\widehat{g_1} = 0$: No skewness present
$\widehat{g_1} < 0$: Negative skewness

Kurtosis gives an information about the shape of the data distribution tails. It measures the tails thickness or "heaviness". A normal distribution has a kurtosis equal three. The 'heavy-tailed' distributions have a kurtosis greater than 3. Contrary, the 'light-tailed' distributions have a kurtosis less than 3. Fig. 30 illustrates three different categories of classification. [18] [16]

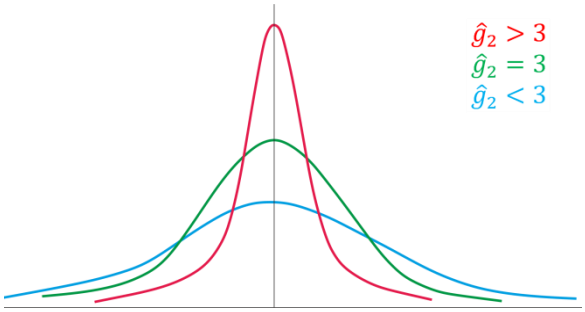

Figure 30. Kurtosis categories. [16]

$\widehat{g_2} > 3$: Leptokurtic distribution, 'heavy-tailed'
$\widehat{g_2} = 3$: Mesokurtic distribution, resembles Normal distribution
$\widehat{g_2} < 3$: Platykurtic distribution, 'light-tailed'

Calculation of kurtosis is given by formula (**33**).

$$\widehat{g_2} = \frac{\sum_{i=1}^{N} \frac{(x_i - \bar{x})^4}{N}}{s^4} \tag{33}$$

Some software programs calculate so called excess kurtosis. Excess kurtosis normalizes the value for normal distribution to zero, simply by subtracting 3 from the kurtosis result. A sharp and lean curve with thicker tails has a positive excess kurtosis, whereas a flatter curve with a lower peak has a negative excess kurtosis.

A great tool to show skewness and kurtosis is the histogram.

Local concentration of data

EA is derived from order statistics, which are ascendingly sorted data elements. Locating the data concentration and their distribution, we use a value P. Value P is also known as order probability and can be calculated in two ways based on data distribution. P is calculated by formula (34) for normal distribution, however, for EA equation given by formula (35) yields better results. [16]

$$P_i = \frac{i - \frac{3}{8}}{n + \frac{1}{4}} \tag{34}$$

$$P_i = \frac{i - \frac{1}{3}}{n + \frac{1}{3}} \tag{35}$$

P-i diagram gives a rough estimate of quantile function Q(P), which is an inverse function to distribution function. [12]

We get a quick overview of data distribution from the mean when we portray so called ridge diagram. The diagram consists of two parts and is separated into two parts at median value. It points out at symmetry, asymmetry resp. and helps us to find outliers. We construct this y-i

diagram accordingly. The median value has order probability P equal 0.5. Data falling below the median are multiplied by 100, see formula (36). Formula (37) computes the residual value from 100 for all data that have P value greater than 0.5. This causes the graph to grow towards the median value. [16]

$$y_i = 100 \cdot P_i, P_i \leq 0.5 \tag{36}$$

$$y_i = 100 \cdot P_i, P_i > 0.5 \tag{37}$$

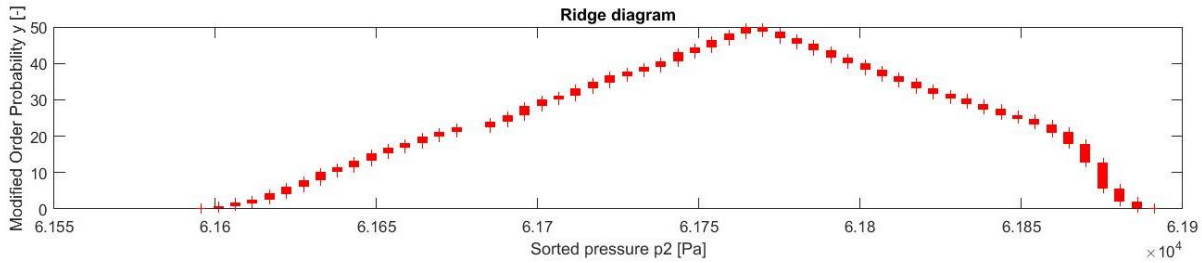

Figure 31. Ridge diagram.

Another way to show the symmetry of data, median value, dispersion around the mean and outliers is a boxplot.

Graphical methods

One of the best known and most used method of visualization is a histogram. Histogram aggregate values and keeps count of their appearance. If the data are unique and repeatedly occur seldom, histogram clusters similar values to so called bins. A bin represents a range of data. Minimum number of bins is dependent on the number of samples and is given by a Sturges' rule. The results for Sturges' given by formula (38) are to be rounded.

$$k = 1 + 3.3 \cdot \log n \tag{38}$$

Where k is the number of bins, and n is the number of samples. [16]

Another way to show data similarity to normal distribution is a P-P diagram. Where a comparison of a cumulative distribution function against cumulative distribution function of normal distribution is shown. The order probability P serves to build the cumulative distribution function of the data set. The more the two lines overlap, the better the data distribution matches the normal distribution. [16]

Similar to the P-P diagram, the Q-Q diagram also shows the comparison of empirical and theoretical distribution. Q-Q stands for 'quantile-quantile' diagram. A quantile from a data set and a theoretical quantile of normal distribution stand against each other. The more they coincide, the closer is the measured data distribution to normal distribution. [10] [11]

While the Q-Q diagrams are more sensitive to data deviation in both ends, the P-P diagrams are more sensitive in the middle range of data.

13 Practical part

13.1 Task one – Steam tables and speed of sound

Thermodynamic properties serve us to calculate the steam velocity and the speed of sound across this region. Both of those velocities are of interest because they allow us to calculate Mach number. At high Mach numbers, the passing medium is being compressed. If the compression is not taken into account, the measured pressures do not match the reality. The coming up error for Pitot-static probe can be calculated with the formula (14).

Determination of thermodynamic properties such as volume of steam *v*, heat capacity ratio *K*, and speed of sound *w* provides a Matlab library IAPWS IF97. This library allows the user to calculate thermodynamic properties within one-phase as well as two-phase region. The chapter Data acquisition discusses the steam tables a little more in depth.

The library allows us to calculate the following thermodynamic properties:

Symbol of thermodynamic property	Name of the thermodynamic property	Units
p	Pressure	MPa
T	Temperature	°C
h	Enthalpy	kJ/kg
s	Entropy	kJ/(kg.K)
v	Specific Volume	m^3/kg
u	Internal Energy	kJ/kg
c_p	Specific isobaric heat capacity	kJ/(kg.K)
c_v	Specific isochoric heat capacity	kJ/(kg.K)
x	Quality of steam	[-]
μ	Dynamic viscosity	Pa.s
η	Kinematic viscosity	m^2/s
λ	Thermal conductivity	W/(m.K)
K	Heat capacity ratio, isentropic coefficient	-
w	Speed of sound	m/s
γ	Surface tension	mN/m

Table 2. Thermodynamic properties of IAPWS IF97 library.

The IAPWS IF97 library uses as inputs specific combination of other thermodynamic properties. I will give here an example of output value of steam volume *v* determined through input values of quality of steam (dryness) *x* and static pressure p_s. More combinations of input values to calculate the output value of steam volume is possible. The other combinations are listed in the Matlab script psteam.m on the attached CD. In a similar fashion are determined the other desired thermodynamic properties.

In the following paragraph, I am going to show a step by step how to activate the library, look for the values of desired thermodynamic property and close the library.

To be able to call the library, we have to open the specific script called psteam.m. The command

```
psteam('open');
```

will serve this purpose. The thermodynamic properties we want to know are density ρ, which is equal to inversed value of volume v, the speed of sound w (in the script denoted as SoS), and the heat capacity ratio K. Before we calculate their values for each point, Matlab advices us to predetermine vector sizes for the thermodynamic properties, e.g. the volume.

```
vol = zeros(size(pS,1),1);
```

where the vector has size(pS,1) rows. It is smart to do because the pS size is given by the measured data itself.

Next step is the look up nomenclature for the steam tables. It generally goes like following

```
psteam('function', parameter 1, par. 2, …)
```

The number of parameters is given by the function itself. One of the ways of input for volume is dryness x and static pressure p_s. Command for volume calculation with parameters x in a range 0 to 1 and p_s in MPa. I use the "for loop" to calculate the value for each point individually.

```
for i = 1:size(pS,1)
    vol(i) = psteam('v_xp',dryness(i),pS(i)*10^-6);
end
```

After gathering all the values of thermodynamic properties, we close the steam table. Easy to guess command follows

```
psteam('close');
```

The other two necessary thermodynamic properties are evaluated within the "for loop", using the same parameters. Last step is to turn the volume into density that is done by inversing the values:

$$\rho = \frac{1}{v}$$

In the previous calculations, we were using dryness, the quality of steam respectively. Its values have to be determined along the blade length. More on data acquisition of quality of steam can be found in chapter Data acquisition section Measurement of steam wetness.

The wetness of the steam is measured on the left side of the turbine set, in front of and behind the last stage blade. The quality of steam, "1 – wetness of steam", along the blade length is portrayed in the pictures below.

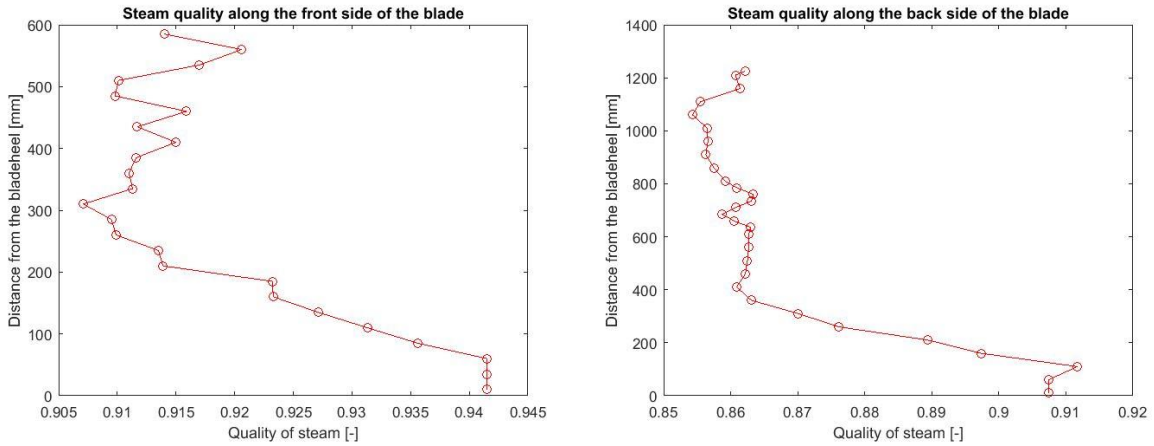

Figure 32. Steam quality in the front and behind the blade.

The quality of steam is highest near the root of the blade because the water droplets drift away due to centrifugal force. The steam quality stays rather constant from 200 mm and farther in front of the blade and from 400 mm farther behind the blade.

Quality of steam *x* in front of the blade reaches: $x = 90.5 \div 94\ \%$

Quality of steam *x* behind the blade reaches: $x = 85 \div 91\ \%$

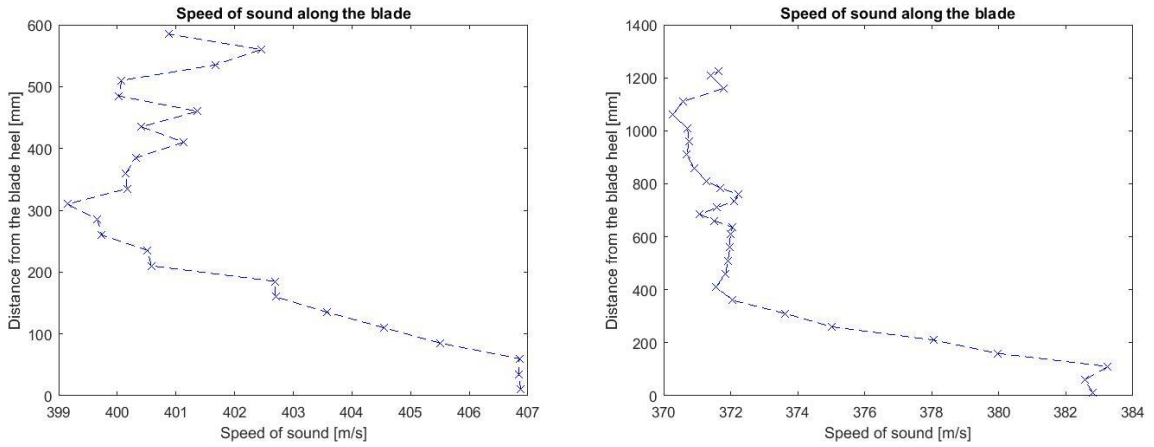

Figure 33. Speed of sound in the front and behind the blade.

The speed of sound in front of the blade reaches up to 407 m/s at the blade root and then slowly decreases. The same progress is recorded behind the blade, however, the speed of sounds reaches maximum of app. 384 m/s.

Speed of sound *SoS* in front of the blade: $SoS = 399 - 407\ m/s$

Speed of sound *SoS* behind the blade: $SoS = 370 - 384\ m/s$

13.2 Task two – Calibration

The processes of calibration takes place before we use the particular probe for data acquisition. Two ways of calibration were mentioned in chapter Calibration. The choice of calibration is made upon the way the data acquisition will be executed.

In our case, we are using the nulling data acquisition, therefore the calibration will be done only for the angle ε. The probe will be turned around a fixed plane parallel to the ground. The probe is moved in -10° and +42° range of the pitch angle. A stand holds the probe in position and takes care of its movement.

During the calibration we record the pitch angle, pressures p_1-p_4, p_B, p_L, p_P, atmospheric pressure p_b and static and total pressures p_{refC} and p_{refS} from a reference Pitot-static probe. All recorded variables lead to creation of calibration coefficients. Calibration coefficients depict the connection between the pressures from different holes and rotation angle ε. Their calculations are constructed according to formula (1). As a reminder

$$k_{\varepsilon_{ij}} = \frac{p_i - p_B}{p_j - p_B} \quad ; i = \{1,2,3,4\}, j = \{1,2,3,4\}, i \neq j$$

Through this calculation, we gather 12 different calibration coefficients for angle ε. Where $k_{\varepsilon_{ij}}$ is the independent variable (axis x) and angle ε is the dependent variable (axis y). According to reference [15], we select only four of those coefficients that have proven themselves, yielding continuously satisfying results. The selected four are coefficients $k_{\varepsilon_{32}}$, $k_{\varepsilon_{12}}$, $k_{\varepsilon_{41}}$, $k_{\varepsilon_{42}}$. They are characterized by no disruptions in the progress and no discontinuations, whilst discontinuation or inflection points affect the other coefficients.

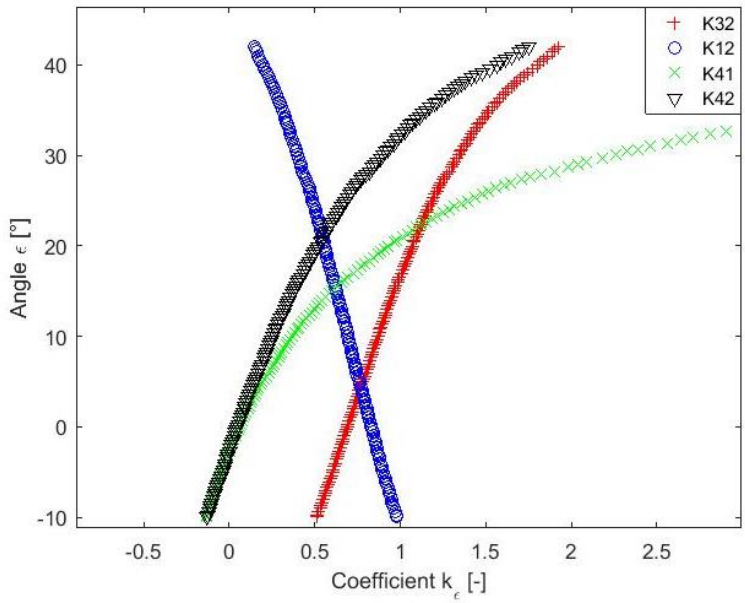

Figure 34. Calibration coefficients.

These issues usually come up as consequence of flow separation or wake. How do these phenomena occur? The following pictures might give a sufficient explanation.

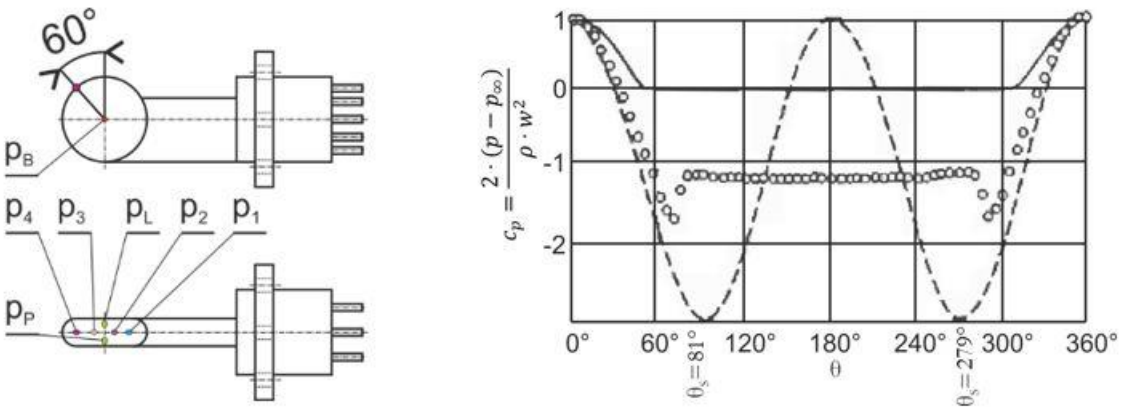

Figure 35. Flow separation, flow about a cylinder at Re = 10^5. [15]

The hole for pressure p_4 can be at certain flow direction located in region that is no longer suitable for gathering data. The region is situated behind an angle of the flow separation. It can be seen in the picture above, where the pressure coefficient c_p is not constant anymore. Once the absolute angle between the hole for p_4 and the incoming flow passes 81°, relative angle –21°, the data are affected by significant flaw and do not hold true. In a similar fashion occurs the discontinuation at relative angle app. -28° as is the case for fig. 12 . The data behind this region are not trustworthy enough. We might use the calibration coefficients only within a certain interval, where no such phenomenon occurs. Nevertheless, we avoid possible issues in the future when we work with appropriate coefficients from the beginning. For further use, only one coefficient is selected. The coefficient $k_{\varepsilon_{32}}$ delivers the best results over different intervals, is monotonous with relatively gradual slope, and no discontinuations and inflection points are present.

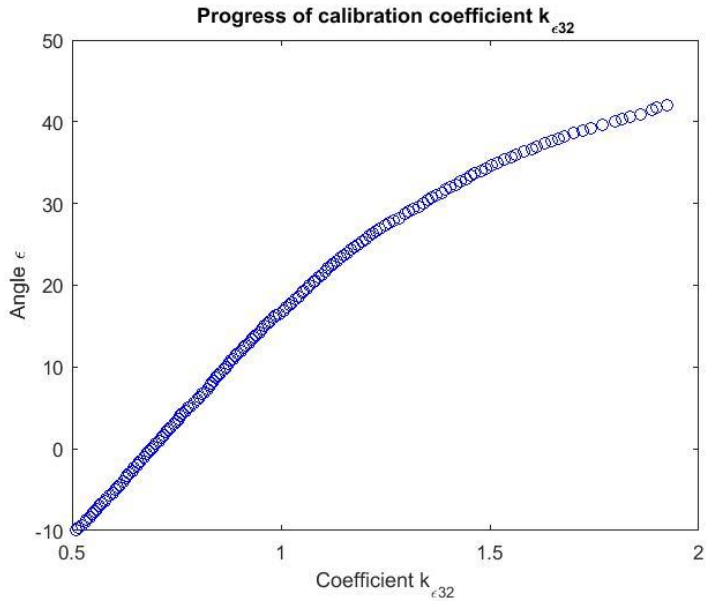

Figure 36. Progress of calibration coefficient $k_{\varepsilon 32}$.

Proper selection of suitable calibration coefficient $k_{\varepsilon_{xy}}$ is followed by determination of static and dynamic pressure coefficients. The static coefficient k_{S_i} and dynamic coefficient k_{D_i} are written out in equations (2) and (3). To refresh our memories:

$$k_{D_i} = \frac{p_i - p_B}{p_{refD}} \quad ; i = \{1,2,3,4\}$$

$$k_{S_i} = \frac{p_i - p_S}{p_{refD}} \quad ; i = \{1,2,3,4\}$$

The coefficients would be impossible to get without the data from a reference probe. The dynamic pressure p_{refD} is a result of difference of total reference pressure and static reference pressure $p_{refC} - p_{refS}$.

We receive another eight calibration curves, four for each.

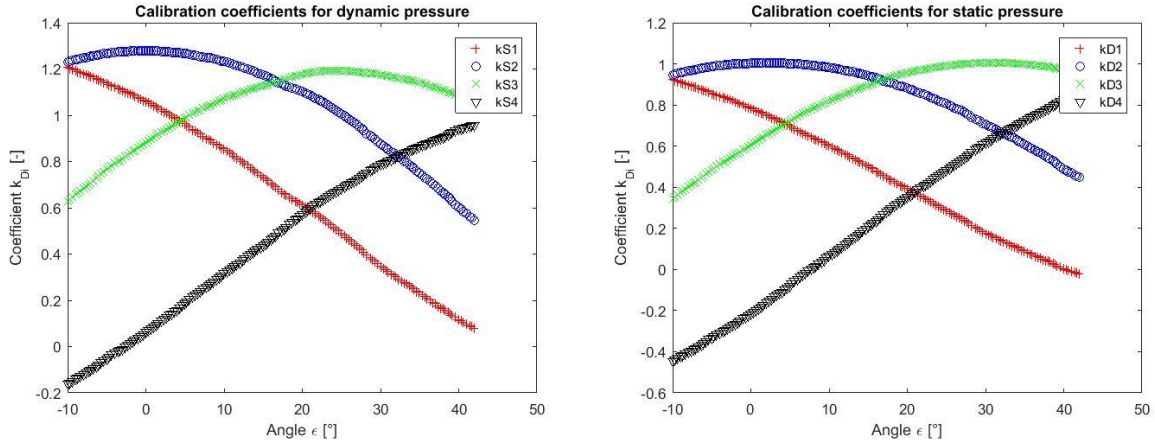

Figure 37. Calibration coefficients for dynamic and static pressure.

Contrary to the coefficients $k_{\varepsilon_{xy}}$, the coefficients k_{D_i} and k_{S_i} are here the dependent variables (axis y) and have the pitch angle as an independent variable (axis x). The desired curves are those that peak at certain point. It is because the curve is the flattest at the peak. Two curves peak in the figure above, the blue curve followed by green curve. Only portions of the curves reaching to their intersection are going to be used further. The selected portions are to see in the fig. 38.

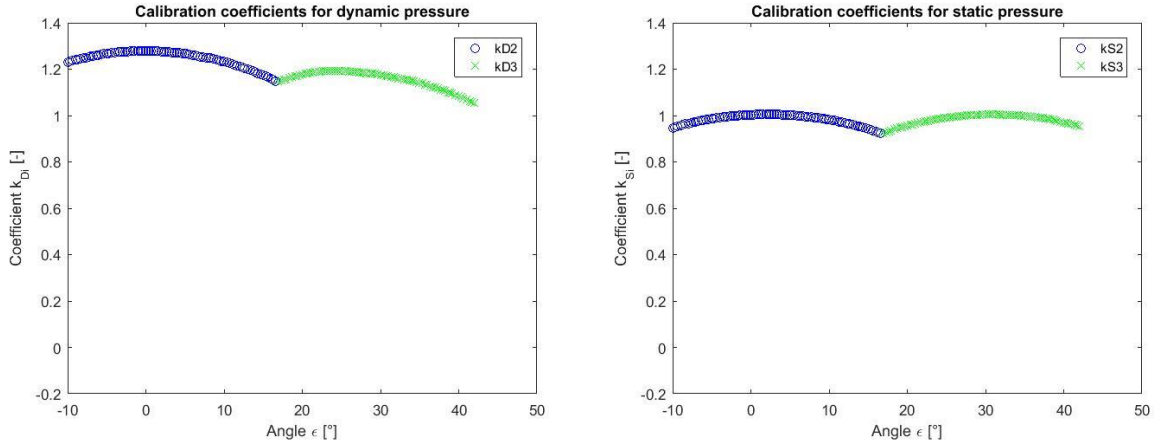

Figure 38. Combined calibration coefficients k_D and k_S for static and dynamic pressure.

Polynomials interpolate the coefficients data, thus creating calibration equations.

13.3 Task three – Calibration equations

Calibration equations give us a mathematical relationship between the coefficients, the measured pressures respectively, and the incoming flow angle ε for an individual probe. A polynomial with high R-squared ensures good enough fit through the data.

For proper fit of calibration data, a curve fitting tool from Matlab is employed. CFtool allows us to pick x and y axis, a curve type and its degree. All those inputs are done manually. I use the polynomial fit. Degree of polynomial depends on the R-squared value. Minimum R-squared to ensure a proper fit is 0.95. I search for a compromise between the R-squared value and the number of degree. When a too high number of a degree were to be picked, it would make the equation excessively and unnecessarily more complicated. Each degree adds another polynomial order and thus next coefficient. In this task, it would not abnormally increase the computing power demand, however, we should apply this concept anyway because the coefficients at the highest orders would be incredibly small. Even though the increase of polynomial degree and R-square goes usually hand in hand, it is not a rule to go by. Sometimes the shape of an eighth degree polynomial curve may seem unrealistic and ridiculous in comparison with a third degree polynomial. Polynomial of higher degree tries to better interpolate all the data including the outliers, therefore, it becomes rather wavy. Once it passes the last data, it takes off to infinity.

Usually only one of the calibration equation is used for further calculations, in our case calibration equation for coefficient k_{32}. Calibration equation for static pressure coefficient k_S consists of two calibration equations. Each within its allocated angle ε interval. Calibration equation of k_{S2} serves for the first interval, where the pitch angle is within ⟨-10°, 16.52°⟩. For the second interval, where the pitch angle is within (16.52°,42°⟩, the calibration equation k_{S3} serves to determine the new static pressure coefficient k_S.

Same interval range and correspondingly similar calibration equations, k_{D2} instead of k_{S2} and k_{D3} instead of k_{S3}, are deployed to determine the new dynamic pressure coefficient k_D.

In the following pictures, I am pointing out properties that are in favor of use and some that are not suitable for any next utilization.

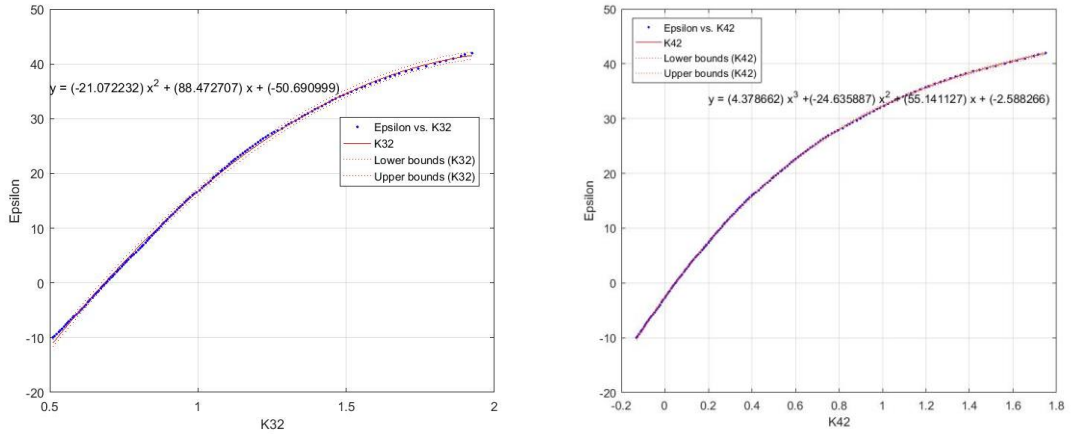

Figure 39. Progress of calibration coefficients K_{32} and K_{42} and their calibration equations.

Both of these progresses are suitable for further use. They both exhibit gradual increase across the whole range of angle ε. Flatter gradual increase is favorable because the accuracy of angle ε is jeopardized less at larger inaccuracies of the coefficient than it would be the case for steep increase. Even though both calibration equations might be used in the next task, I select the calibration equation for calibration coefficient K_{32}. It is because coefficients with indices 1 and 4, pressures p_1 and p_4, respectively are not recommended due to their higher possibility to end up behind the flow separation point. It would then lead to sudden changes in coefficient. More about this in chapter 5.

The next two figures depict calibration coefficients that exhibit properties that are not wanted. Such as a fast rising/falling curve or a calibration equation that even at high orders does not copy the point trajectory well. The fast rising/falling curve is not suitable because it is more sensitive to deviations of the input values than moderately rising/falling curves.

The calibration equation is simply not accurate enough compared to the two solutions above. If you wanted to use necessarily this calibration coefficient, you would have to crop all the point of the 'tail' and fit a new curve through the limited number of points.

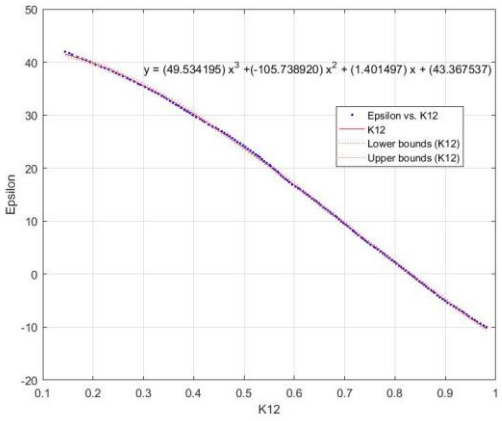

Figure 40. Fast falling progress of calibration coefficient K_{12}.

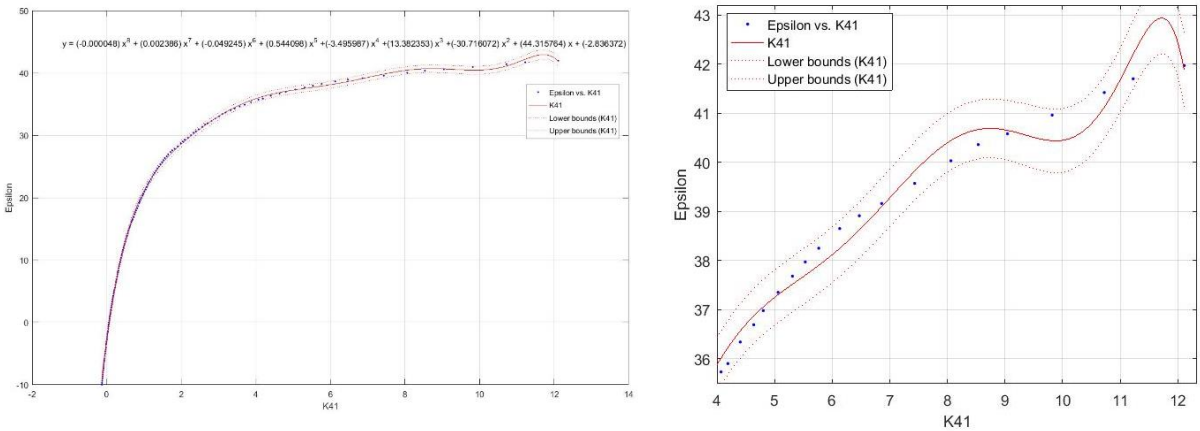

Figure 41. Progress of calibration coefficient K_{41} and its problematic tail.

Here we have four calibration equations for coefficients K_{12}, K_{32}, K_{41}, and K_{42}.

Coefficient	x^8	x^7	x^6	x^5	x^4	x^3	x^2	x^1	x^0
K_{32}							**-21.07**	**88.47**	**-50.69**
K_{12}						49.53	-105.7	1.401	43.37
K_{41}	$-4.78*10^{-5}$	$2.39*10^{-3}$	$4.93*10^{-2}$	$5.44*10^{-1}$	-3.50	13.38	-30.72	44.32	-2.84
K_{42}						4.38	-24.64	55.14	-2.59

Table 3. Calibration equations' coefficients.

The calibration equation K_{32} is used for determination of angle ε from the new pressures that are measured at the last stage of a turbine. Angle ε cannot be measured during the data acquisition because the steel stem cannot tilt to a side. Yaw angle at this point changes so the condition $\Delta p = p_L - p_p = 0$ is fulfilled. The steel stem can be rotated around its axis. More about probe nulling in the chapter Nulling of the probe.

Calibration coefficients for static and dynamic pressure are put together from two different calibration coefficients k_{S2} and k_{S3} or k_{D2} and k_{D3}. To see it, refer please to fig. 38 . The joint of the two progresses leads to different calibration equation for each portion. You can read up more about the joint in Task two – Calibration.

The different calibration equations are depicted in the picture 42. Each equation is used for different interval based on value of angle ε. Note: Angle ε is calculated from calibration equation for K_{32}.

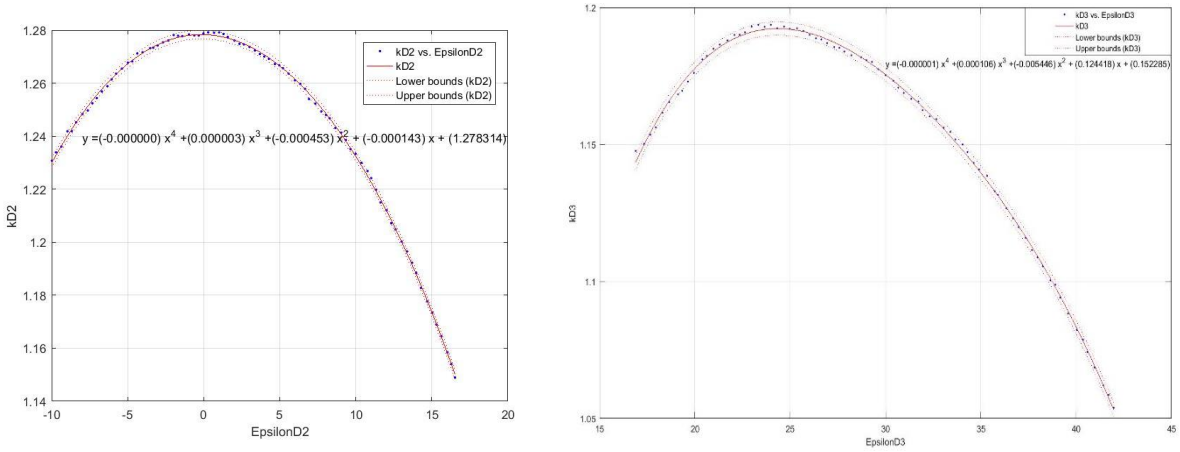

Figure 42. Calibration equation for dynamic pressure k_D via calibration equations of k_{D2} and k_{D3}.

Coefficient	ε Interval	x^4	x^3	x^2	x^1	x^0
k_{D2}	⟨-10°, 16.52°⟩	$-1.91*10^{-7}$	$2.68*10^{-6}$	$-4.53*10^{-4}$	$-1.43*10^{-4}$	1.28
k_{D3}	(16.52°, 42°⟩	$-8.25*10^{-7}$	$1.10*10^{-4}$	$-5.45*10^{-3}$	$1.24*10^{-1}$	$1.52*10^{-1}$

Table 4. Calibration equations' coefficients.

Dynamic pressure p_D of the measured data from turbine is calculated by formula (4). One of the component is the calibration coefficient k_D that is calculated through the calibration equation based on the angle ε.

In a similar manner is proceeded to calculate for static pressure p_S. This time only via formula (5).

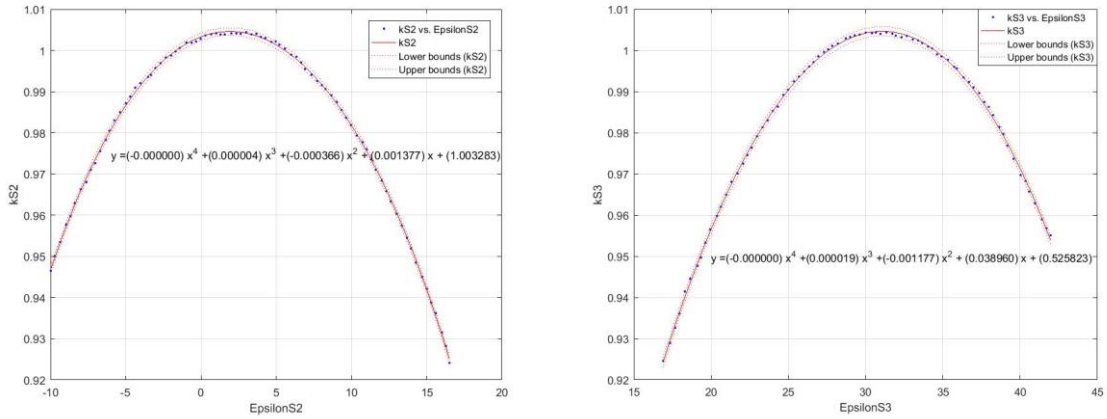

Figure 43. Calibration equation for static pressure k_S via calibration equations of k_{S2} and k_{S3}.

Coefficient	ε Interval	x^4	x^3	x^2	x^1	x^0
k_{S2}	⟨-10°, 16.52°⟩	$-2.45*10^{-7}$	$3.79*10^{-6}$	$-3.66*10^{-4}$	$1.38*10^{-3}$	1.00
k_{S3}	(16.52°, 42°⟩	$-1.62*10^{-7}$	$1.85*10^{-5}$	$-1.18*10^{-3}$	$3.90*10^{-2}$	$5.26*10^{-1}$

Table 5. Calibration equations' coefficients.

13.4 Task four – Flow parameters

In this task we discuss the distribution of static pressure p_S, dynamic pressure p_D, and total pressure p_C over the blade length. We calculate the distribution of velocity components of the steam over the blade length as well.

Data are measured in two different places of the Temelín LP turbine: in the front of the last-stage blade on the left side and behind the last-stage blade on the left side.

Data in front of the last stage are acquired along the blade at these distances from the blade root. At total number of 25 points.

Distance from root [mm]	Distance from root [mm]	Distance from root [mm]	Distance from root [mm]	Distance from root [mm]
10	135	260	385	510
35	160	285	410	535
60	185	310	435	560
85	210	335	460	585
110	235	360	485	610

Table 6. Measuring distances at the front blade.

Data behind the last stage blade are collected over greater number of points. In the table below, you can see the exact values.

Distance from root [mm]	Distance from root [mm]	Distance from root [mm]	Distance from root [mm]	Distance from root [mm]
10	360	660	860	1210
60	410	685	910	1225
110	460	710	960	1240
160	510	735	1010	1255
210	560	760	1060	
260	610	785	1110	
310	635	810	1160	

Table 7. Measuring distances at the back blade.

At these points we measure all seven pressures from the probe, p_1, p_2, p_3, p_4, p_B, p_L and p_P, yaw angle, where the condition $\Delta p = p_L - p_p = 0$ is successfully completed and we keep track of the atmospheric pressure p_b.

From the measured pressures p_2, p_3, p_B we calculate new pressure coefficient K_{32}. For the calibration coefficient K_{32} we have built a calibration equation in calibration tasks two and three. The new pressure coefficient K_{32} is then plugged into the calibration equation to yield values for incoming angle ε of the steam. For this, a Matlab built-in function feval is used.

```
Eps32 = feval(fitresults{1}, K32);
```

Where Eps32 is the calculated angle ε, fitresults{1} and K32 are parameters of the function feval, fitresults{1} is the calibration equation for K_{32}, K32 is the new pressure coefficient.

Next step is to determine values of coefficient for static and dynamic pressure k_S and k_D. Both coefficients are calculated from the appropriate calibration equation and pitch angle

determined in the past task. The value of angle ε defines which of two calibration equations kD2 or kD3, kS2 or kS3 resp., is going to be used. If the angle ε is less or equal 16.52°, the kD2, correspondingly kS2 calibration equation is going to be employed. If the angle ε is greater than 16.52°, kD3, correspondingly kS3 is going to be utilized.

Example of command for kD2 calculation:

kD2 = feval(fitresults{5}, Eps32);

Where calibration equation for kD2, denoted fitresults{5}, and angle ε, denoted Eps32, are parameters of feval function.

So via calibration equations and angle ε we receive two coefficients for static and dynamic pressure k_S and k_D. Those coefficients are components to formulas for calculation of dynamic and static pressures.

Dynamic pressure is calculated by formula (4) that reads

$$p_D = \frac{p_3 - p_B}{k_D}$$

Static pressure can be calculated by formula (5) that reads

$$p_S = p_i - \frac{k_S}{k_D} \cdot (p_i - p_B),\ p_S = p_i - k_S \cdot p_D \text{ resp.}$$

Sum of static and dynamic pressure yields total pressure p_C.

$$p_C = p_S + p_D$$

The steam pressures are used to find velocity components of the steam. The velocity vectors are shown here in the figure 13.

For velocity calculation given by formula (8)

$$c_2 = \sqrt{\frac{2 \cdot \kappa}{\kappa - 1} \cdot \frac{p_S}{\varrho} \cdot \left(\left(\frac{p_C}{p_S} \right)^{\frac{\kappa - 1}{\kappa}} - 1 \right)}$$

Variables such as heat capacities ratio κ, static pressure p_S, total pressure p_C and density ρ has to be determined first. The pressures are successfully found out, but the other two variables κ and ρ are still missing. To determine those, library of thermodynamic properties IAPWS – IF97 is going to be used. More about the library and how it is operated can be found in Task one – Steam tables and speed of sound. Both variables are calculated through a specific function with several parameters. In our case, the parameters are static pressure p_S and quality of steam x, dryness respectively. Quality of steam over the blade length is shown in task one. Commands below call a specific function from the library through two of its parameters.

vol(i) = psteam('v_xp',dryness(i),pS(i)*10^-6);

kappa(i) = psteam('ka_xp',dryness(i),pS(i)*10^-6);

Dryness = Quality of steam is given as a decimal number, not percentage and static pressure is given in MPa.

Density is then calculated as an inverse value of wet steam volume.

$$\rho = \frac{1}{vol}$$

The calculated speed can be taken apart to three orthogonal vectors in directions r - radial, u - tangential, and z – axial, as shown in the fig. 13 . Formulas (9), (10) and (11) are put in use for calculation of the speed components.

Now we are going to look at and compare the calculated variables in the front and behind the last-stage blade.

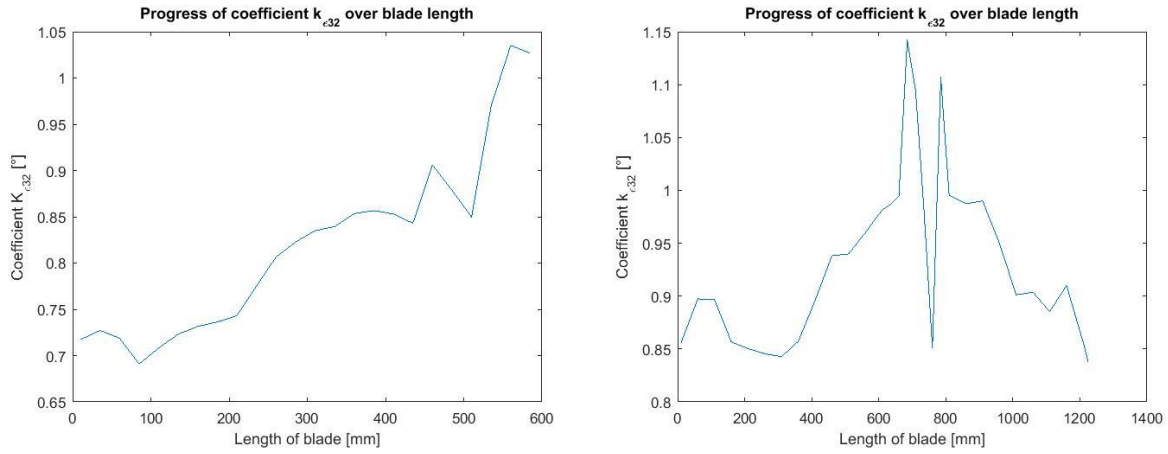

Figure 44. Coefficient K_{32} in the front of the blade [left] and behind the blade [right].

The coefficient K_{32} in the front of the blade gradually increases along the blade. Contrary to this, the progress of the coefficient behind the blade is inconsistent. The coefficient has a rather growing trend at the beginning, and then becomes rocky around the 700 mm mark, where a deep drop suddenly occurs. That could be due to location of a tie-boss, a stabilization device, on the blade. The flow in its vicinity gets disturbed. The coefficient then spikes up again, followed by gradual decrease. The value of K_{32} in the front ranges from 0.7 to 1.05 and K_{32} behind ranges from 0.85 to 1.15. This means, when plugged into the calibration equation, the angle ε of the incoming steam is larger behind the blade.

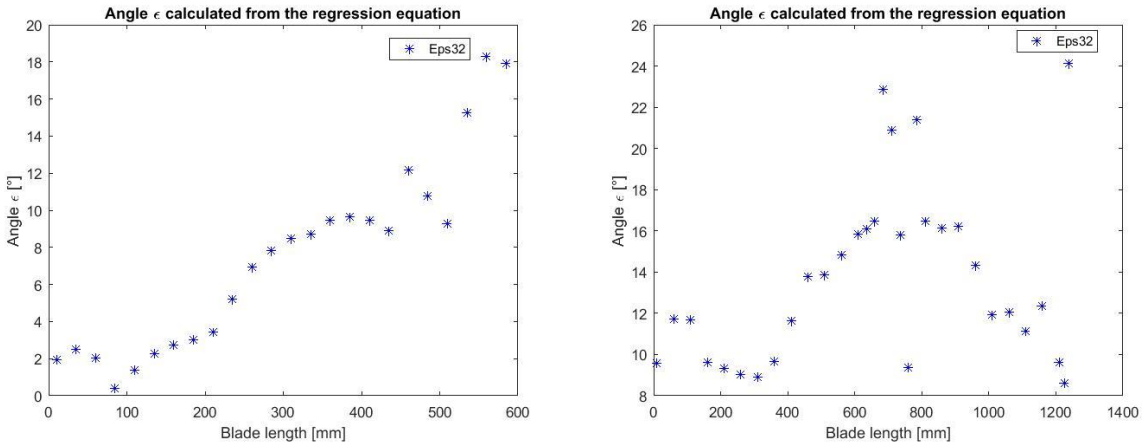

Figure 45. Angles ε of the incoming steam in the front [left] and behind [right] the blade.

The progression of angle ε copies the shape of the coefficient K_{32}. The angle ε in the front moves within 0° and 18°, behind the blades within 8° and 24°.

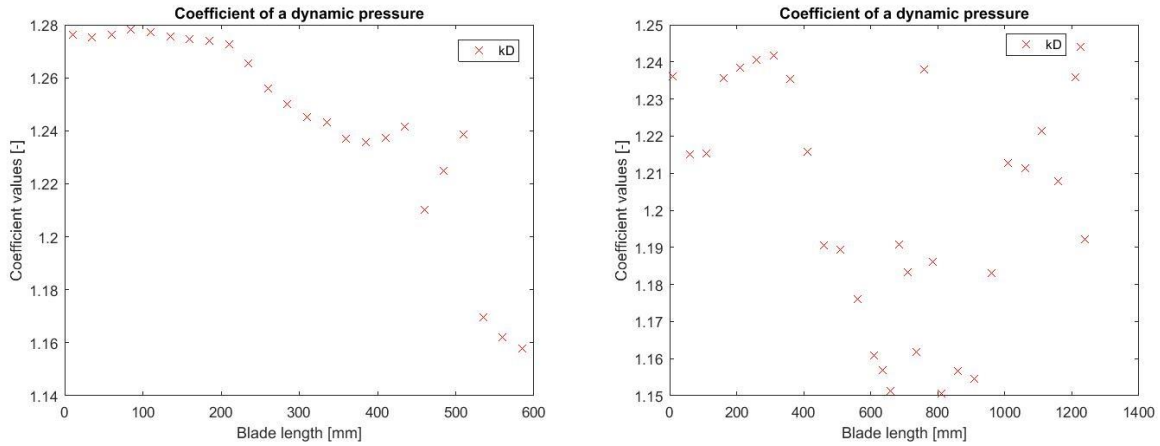

Figure 46. Coefficients of a dynamic pressure in the front [left] and behind [right] the blade.

The coefficient k_D in the front of the blade stays rather constant at the beginning, around 200 mm k_D slowly drops. At 400 mm and further the coefficient seems inconsistent. Altogether is the progression quite constant because the coefficient moves only within the values 1.14 and 1.28.

Behind the blade seems the coefficient k_D irregular, fast changing and inconsistent. The sudden increase after the drop is caused by tie-boss that is located in about 700 mm on the blade. The flow is subsequently disrupted as well as pressures and other pressure dependent variables. The shape of the coefficient across the blades forms the letter "W". Overall is the coefficient again very stable. I say this because it fluctuates only within the 1.15 and 1.25 boundaries.

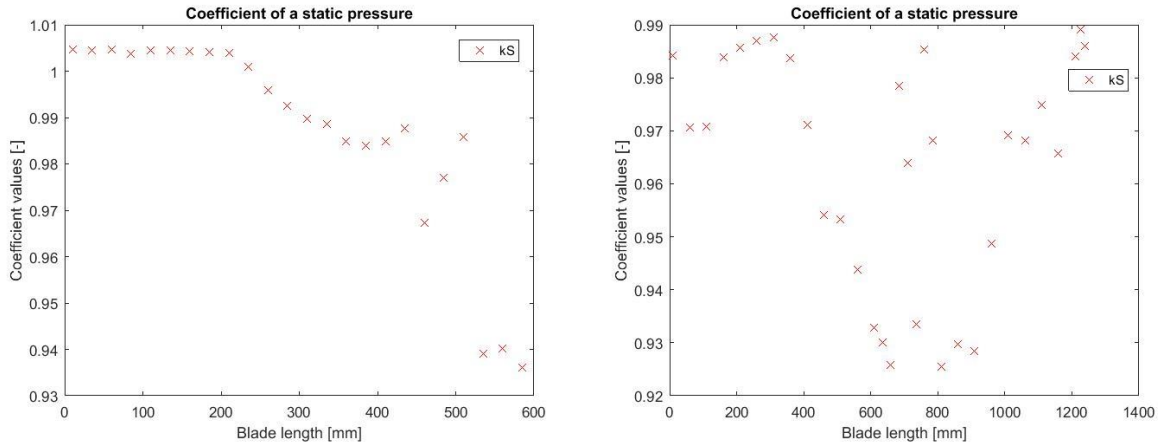

Figure 47. Coefficients of a static pressure in the front [left] and behind [right] the blade.

The coefficients k_S in the front as well as behind the blade are in their shape similar to the coefficients k_D. The only difference is the range of both coefficients. Whereas the coefficient in the front of the blade rises and falls within 0.93 and 1.01, the coefficient behind the blade oscillates within 0.92 and 0.99.

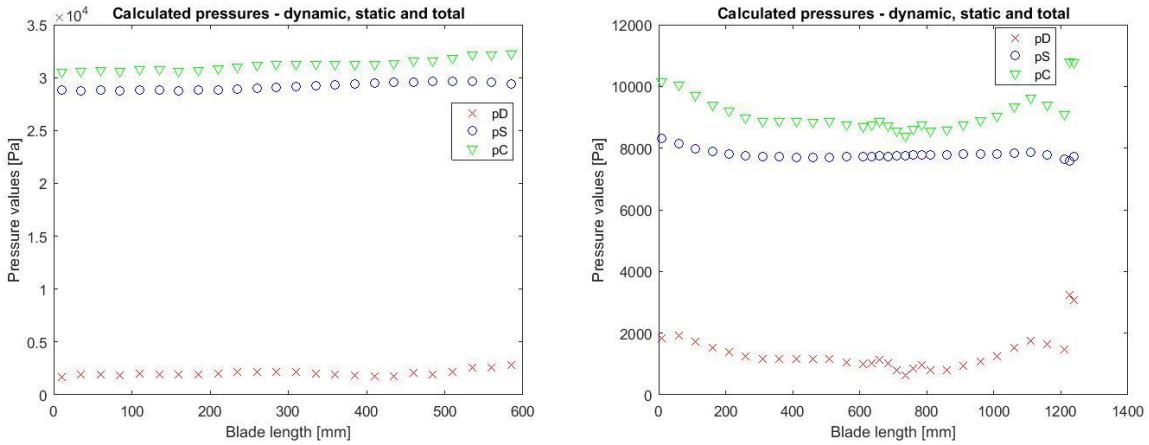

Figure 48. Calculated total, dynamic and static pressures at the front and back blade.

Before the steam hits the last-stage blade, the static pressure p_S and therefore the total pressure p_C are still relatively high in comparison with the pressures in condenser. The median values of pressures are written out below:

Static pressure: $p_S = 29150\ Pa$

Dynamic pressure: $p_D = 1984\ Pa$

Total pressure: $p_C = 31249\ Pa$

While the steam is working on the blade, it expands and simultaneously the pressure drops. The pressure should be therefore much closer to the condenser pressure. The median pressure values are written out below:

Static pressure: $p_S = 7752\ Pa$

Dynamic pressure: $p_D = 1161\ Pa$

Total pressure: $p_C = 8882\ Pa$

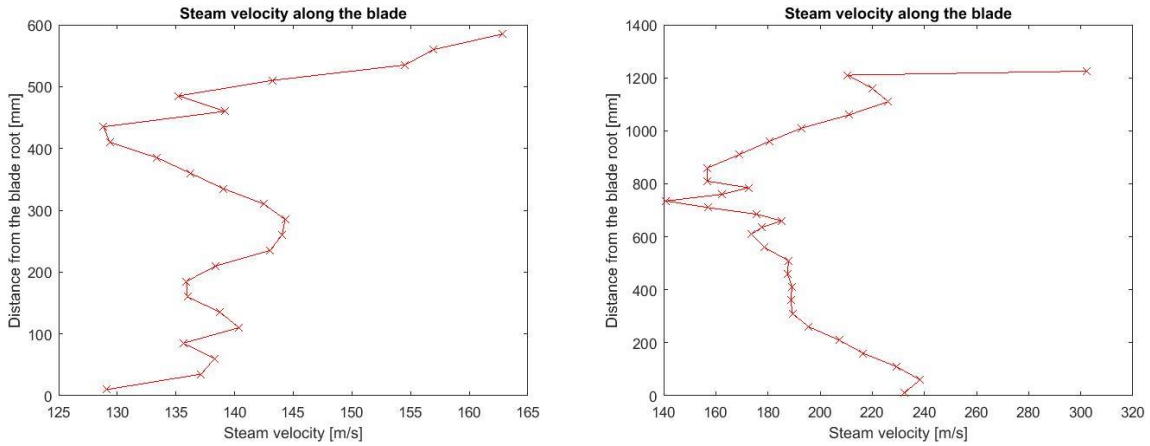

Figure 49. Steam velocity development along the blade length. In front of [left] and behind [right] the blade.

Velocity of steam in the front of the blade varies along the blade length. At the blade root, the speed is app. 130 m/s and then it unevenly rises and falls, creating zigzag pattern. At around 300 mm mark the speed reaches its local maximum with speed app. 145 m/s. Sudden drop to the original 130 m/s at 400 mm, followed by an increase up to 163 m/s.

Speed in front of the blade ranges from 129 to 163 m/s.

Different behavior of the steam can be seen behind the blade. The steam speed at the root is high, reaching 230 m/s. It shortly spikes but then gradually decreases to around 140 m/s in about 730 mm distance from the root. At this point, the steam starts to speed up again up to app. 230 m/s. The last point shows the steam speed about 300 m/s, which seems unreasonably high. This seems to be the consequence of the rigged measured pressures. The pressures deliver abnormal values at the end of the blade.

Speed behind the blades ranges from 141 to 238 m/s.

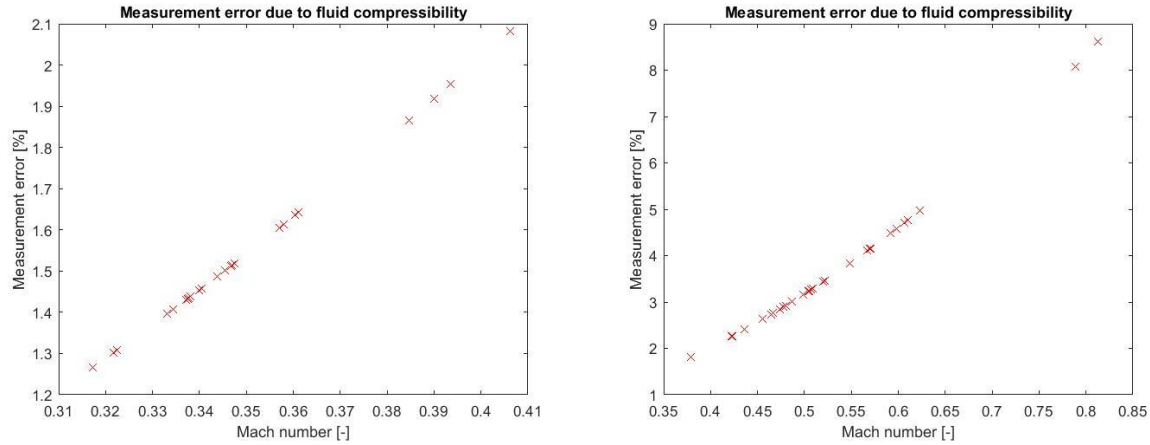

Figure 50. Measurement error due to fluid compressibility in front of [left] and behind [left] the blade.

Part of this task is to determine the measurement error due to steam compressibility. From the task above, we calculated the steam velocity. In order to determine the Mach number, a speed of sounds has to be determined.

The speed of sound is calculated from thermodynamic tables IAPWS-IF97 as a function of two parameters, quality of steam x and static pressure p_S. Mach number is then calculated by the formula given below.

$$Ma = \frac{c}{SoS} \tag{39}$$

Where c is the steam velocity and SoS is the speed of sound.

Mach number behind the penultimate stage reaches from 0.31 to 0.41 Ma. The measurement error reads from 1.2 to 2.1 percent. This number is not so significant in comparison with the error behind the last stage blade. The Mach numbers are higher which implies the measurement errors are going to be higher as well. Mach numbers range within 0.35 and 0.85 Ma. The measurement error reaches up to 9 %, which should not be overlooked and could significantly change the results of other calculated values based on those pressures.

We may notice that the progression is not linear, rather squared. And it is so, the formula (14) contains Ma^2.

13.5 Task five – Uncertainty of measurement

We calculate the uncertainties of all measured and calculated variables present in task four. Every set of data is measured with certain level of confidence and no measuring instrument is able to measure flawlessly. We look at the data with certain doubt. We try to turn this doubt into numbers, usually of the same units as the measured value. There are two types of uncertainties and for each different approach is taken. Uncertainty of type A is estimated from statistics of the dataset. Calculation of type B uncertainty is based on calibration certificates of the OEM. These two uncertainties are combined together, which gives the final uncertainty of the variable.

All the calculations we do here, come from the measurement of the pressures in the turbine. In chapters 3 and 4 we discuss what equipment we use to measure them. Pressure transmitter ROSEMOUNT type 3051S measures the atmospheric pressure nearby turbine. According to its data sheet, the guaranteed ROSEMOUNT's error is not larger than 0.035 % of FS. The full scale equals to 207 kPa, giving us the limit value of error for atmospheric pressure 72.45 Pa. Pressure transducer NETScanner 9116 records the relative pressures of the probe with high accuracy. Nevertheless, it gives an error as well. The error given in the manufacturer's data sheet says 0.15 % of FS. The full scale for this channel equals 15 Psi or 103421 Pa. The error for measured relative pressures equals about 155.13 Pa. Both of these errors are type B errors.

Three pressures p_2, p_3 and p_B are input values for determination of coefficient K_{32} and other formulas and tables used for calculation of static and dynamic pressure and steam speed. Combined uncertainty, see formula (22), is the root sum of the squares of type A and type B uncertainties. How to receive the type B uncertainty is explained in the paragraph above. Type A is calculated by formula (20). The results are equal to a standard deviation divided by the square root of number of elements in the data set. We calculate the combined uncertainty for each measured pressure individually. Calculation of combined uncertainty for an atmospheric pressure p_b is also necessary. The three absolute pressures p_2, p_3 and p_B consist of the atmospheric pressure and the reference pressure. We assume the data have normal distribution. We multiply the combined uncertainty by coverage factor C equal 2 that ensure the confidence level to be 95 %.

Pressure	Expanded uncertainty in the front of the blade [Pa]	Expanded uncertainty in the back of the blade [Pa]
p_b	144.90	144.90
p_B	310.49	310.40
p_2	310.58	310.62
p_3	310.82	310.14

Table 8. Expanded combined uncertainties.

The uncertainties of type B are dominant over the type A.

This uncertainty is added to and subtracted from the measured values of pressures p_2, p_3, p_B. Thus, we calculate the upper and lower limit of each variable. The combination of only upper and only lower limits is then used to calculate the coefficient K_{32}. Now, we have two sets of data for coefficient K_{32}. Both coefficients are now inputs for the K_{32} regression equation to calculate the angle ε. We do have again two sets of data for angle ε. Angle ε is an input for static and dynamic coefficients regression equations. Like this we receive four coefficients,

the upper and lower limit for the dynamic coefficient k_D and the upper and lower limit for the static coefficient k_S.

Static and dynamic pressures are calculated again individually for the upper and the lower limit.

In front of the blade

Dynamic pressure uncertainty: 19.7 Pa

Dynamic pressure has a relative uncertainty 0.937 %.

Static pressure uncertainty: 455.4 Pa

Static pressure has a relative uncertainty 1.760 %.

Behind the blade

Dynamic pressure uncertainty: 22.1 Pa

Dynamic pressure has a relative uncertainty 1.08 %.

Static pressure uncertainty: 465.3 Pa

Static pressure has a relative uncertainty 5.416 %.

In steam tables IAPWS - IF97 we look for the values of volume, speed of sound and heat capacity ratio *K* through their functions and parameters. The parameter values are again static pressure and steam quality. Since there are two limits of static pressure, there are again upper and lower limits for each of the variables.

The final step is to determine the uncertainty of the steam velocity *c*. The progression of the steam velocity and its upper and lower limits is shown below.

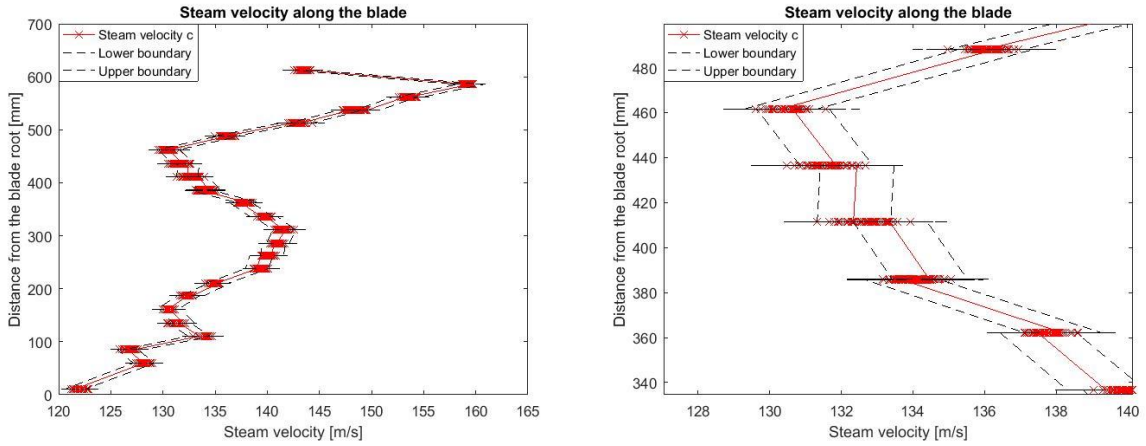

Figure 51. Steam velocity and its uncertainty in the front blade, Close-up [right].

The steam velocity ranges from about 120 to 160 m/s. At the blade root, the velocity starts at about 120 m/s and then increases to over 140 m/s at 300 mm mark. Then starts to drop

towards 130 m/s at 460 mm blade length. Then a rapid increase happens and the steam velocity reaches its peak at 160 m/s. At the top of the blade the speed velocity suddenly drops. The upper and lower boundaries show the steam uncertainty in the front blade.

On the right side, there is a close-up to a 460 mm mark. The dashed lines show the uncertainty of the measurement, which is about 1.26 m/s at a level of confidence of 95 %. The relative uncertainty has a value of 0.792 %.

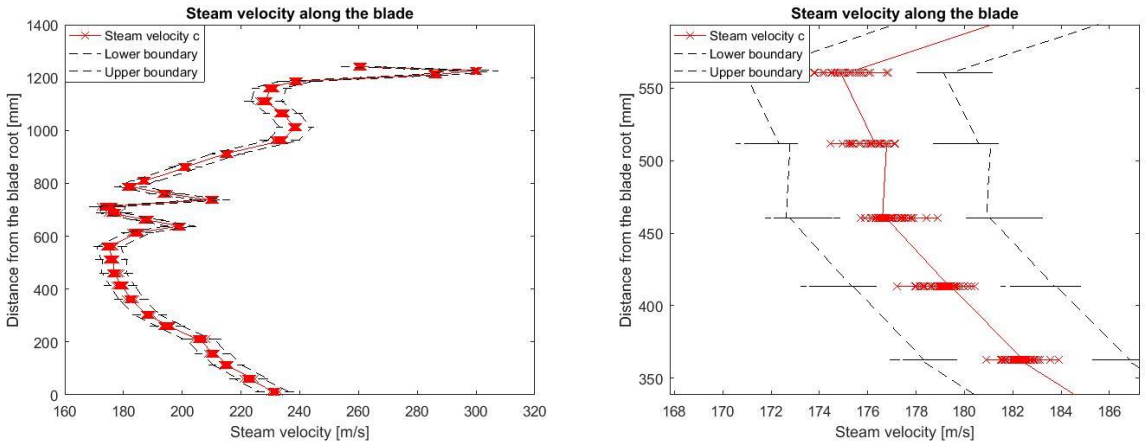

Figure 52. Steam velocity and its uncertainty behind the blade, Close-up [right].

In the fig. 52, there is the steam velocity distribution along the blade. The velocity ranges from 170 m/s to a little over 300 m/s. The right hand side of the figure shows a close up of the 500 mm mark. Two dashed lines represent the uncertainty of the velocity. The absolute velocity uncertainty equals to 6.85 m/s, in relative units, it is equal to 2.29 % of the steam speed.

The absolute and relative uncertainty of the steam velocity and its components are presented in table below.

Steam component	Expanded uncertainty in the front of the blade		Expanded uncertainty in the back of the blade	
	Δy	Relative	Δy	Relative
c	1.26 m/s	0.792 %	6.85 m/s	2.29 %
c_u	0.417 m/s	0.814 %	3.81 m/s	2.33 %
c_z	1.18 m/s	0.796 %	5.68 m/s	2.92 %
c_r	0.458 m/s	0.796 %	4.08 m/s	2.34 %

Table 9. Absolute and relative uncertainties of steam velocity and its components.

13.6 Task six – Statistics

Statistical analysis of data give us the notion what data set we are dealing with. For purpose of this thesis, we are going to use exploratory analysis of one-dimensional data. Graphical methods of exploratory data analysis are used for complex evaluation of statistical peculiarities of data.

In the measured data, we are trying to identify pattern of periodicity and data trends. We do it because a data set with presence of trends does not comply with the normality condition, thus the results of the common analysis tools are not reliable. Close ups of data distribution of pressure p_2 are given below. Confident bands and predictions bounds are given below as well, showing a dispersion and expected positions of pressure p_2 true values.

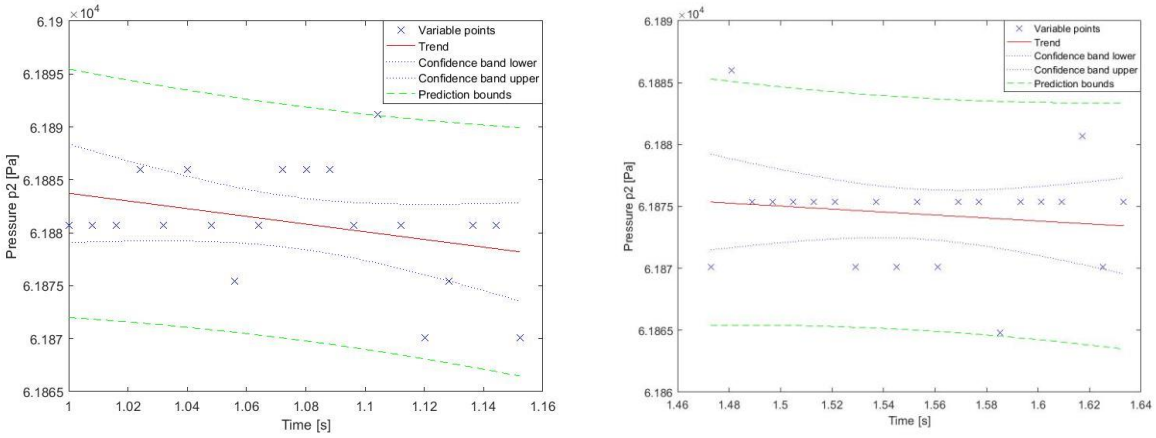

Figure 53. Close-ups of data distribution at two random places of pressure p_2 progress.

None of the picture records any trends or recurring changes in trends or harmonic behavior. Hence, we may assume the data are suitable for further use.

Location and scale parameters

Mean, median and mode are the basic indicators of data distribution. Just knowing their values gives us a solid overview what the distribution looks like. More about statistics in the chapter Statistics.

Mean also referred to as the average of the data set. It is equal to sum of the data points divided by the number of data points.

$$\bar{x} = \sum_{i=1}^{N} \frac{x_i}{N}$$

$$\boldsymbol{\bar{x} = 61763\ Pa}$$

The mean value for our randomly selected pressure p_2 data set equals to 61763 Pa.

Median value from the data set where half of the data values are below this value and half above.

$$\bar{x} = x_{\left(\frac{N+1}{2}\right)} \; if \; N \; is \; odd$$

$$\bar{x} = \frac{x_{\left(\frac{N}{2}\right)} + x_{\left(\frac{N}{2}-1\right)}}{2} \; if \; N \; is \; even$$

$$\boldsymbol{\bar{x} = 61767 \; Pa}$$

The median value is calculated via the second formula because the data set has 500 samples. The formula gives result 61767 Pa. The median value is slightly higher than the mean.

Mode is the most frequently occurring value from the dataset. It is easy to see in histogram. Mode is the midpoint of the highest peak.

$$\boldsymbol{\bar{x} = 61875 \; Pa}$$

The most frequently occurring value of a data set is equal to 61875 Pa. Which is slightly higher than the mean and median.

In normal distribution fall mean, median and mode together. This is, however, not the case for any other distribution or even slight deviation from normal distribution. [4]

The more mean and median differ, the more it points out at nonnormality of the data. The difference between the mean and the median can be expressed as absolute difference between the two values or in relative difference to the mean.

$$Diff_{abs} = |Mean - Median|$$

$$Diff_{rel} = \frac{|Mean - Median|}{Mean}$$

$$\boldsymbol{Diff_{abs} = 4.03 \; Pa}$$

$$\boldsymbol{Diff_{rel} = 6.52 \cdot 10^{-5}}$$

Both differences are very small. The relative difference falls below 0.1, the data set is ruled out as **normal**.

Variance s^2 gives us the information how disperse the data in the data set are. [5]

$$s^2 = \sum_{i=1}^{N} \frac{(x_i - \bar{x})^2}{N-1}$$

Where $\bar{x}$ is the mean of the data, N is the number of elements in the data set.

$$\boldsymbol{s^2 = 7692 \; Pa^2}$$

The variance of the data set is calculated via the formula above and is equal to 7692 Pa^2.

Standard deviation is the square root of the variance. The units of spread again match the original data, which is not the case for variance. [5]

$$s = \sqrt{\sum_{i=1}^{N} \frac{(x_i - \bar{x})^2}{N-1}}$$

$$\boldsymbol{s = 87.7\ Pa}$$

Standard deviation of the data set stands at 87.7 Pa.

Range, the distance between the largest and smallest data set value, is equal to **295.6 Pa**.

Skewness and kurtosis

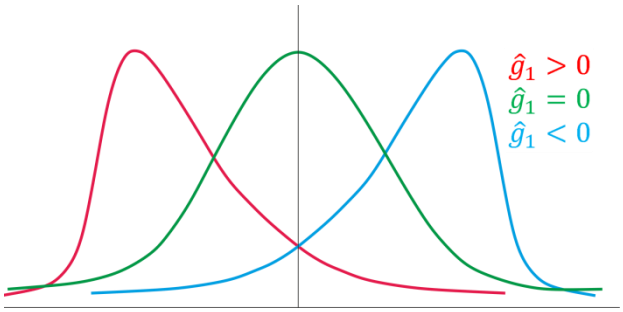

Figure 29. Data distributions and their skewness coefficient values from Fisher-Pearson. [16]

$$\boldsymbol{\widehat{g_1} = -0.188}$$

Skewness $\widehat{g_1}$ is equal to -0.188 and apparently the data set has a negative skewness. The data are skewed slightly to the left. The majority of the data are accumulated on the right side. This also complies with the characteristics that mean is less than median and both are less than the mode.

Kurtosis gives an information about the shape of the data distribution tails. It measures the tails thickness or heaviness. Figure below illustrates three different categories of classification.

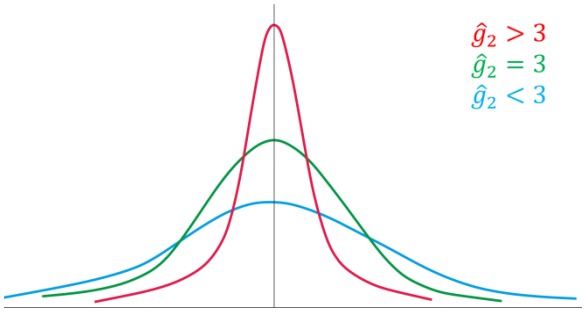

Figure 30. Kurtosis categories. [16]

Calculation of kurtosis is given by

$$\widehat{g_2} = \frac{\sum_{i=1}^{N} \frac{(x_i - \bar{x})^4}{N}}{s^4}$$

$$\boldsymbol{\widehat{g_2} = 1.73}$$

Kurtosis value is determined through Matlab calculation and gives result 1.73, which indicates the platykurtic, more spread out, distribution with "light" tails.

Local concentration of data

Ridge diagram with modified order probability is quick way to show the median value of the data set. The diagram points out symmetry, asymmetry resp. of the data and its outliers.

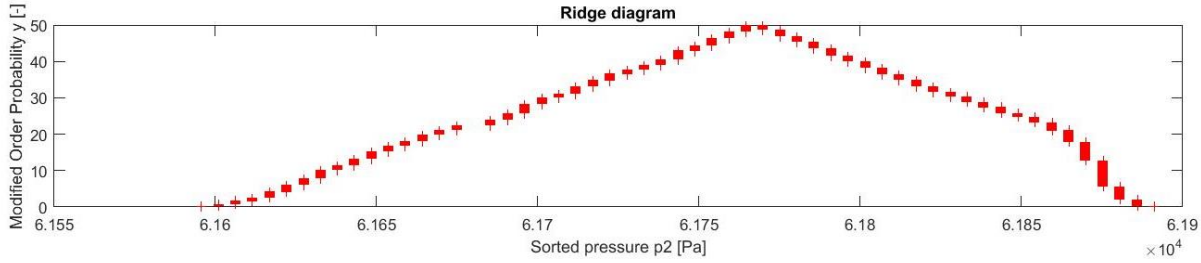

Figure 54. Ridge diagram.

The highest modified order probability marks the median value. **Median** value is equal to **61767 Pa**.

Boxplot is another great way to show the symmetry of data, median value, dispersion around the mean and outliers.

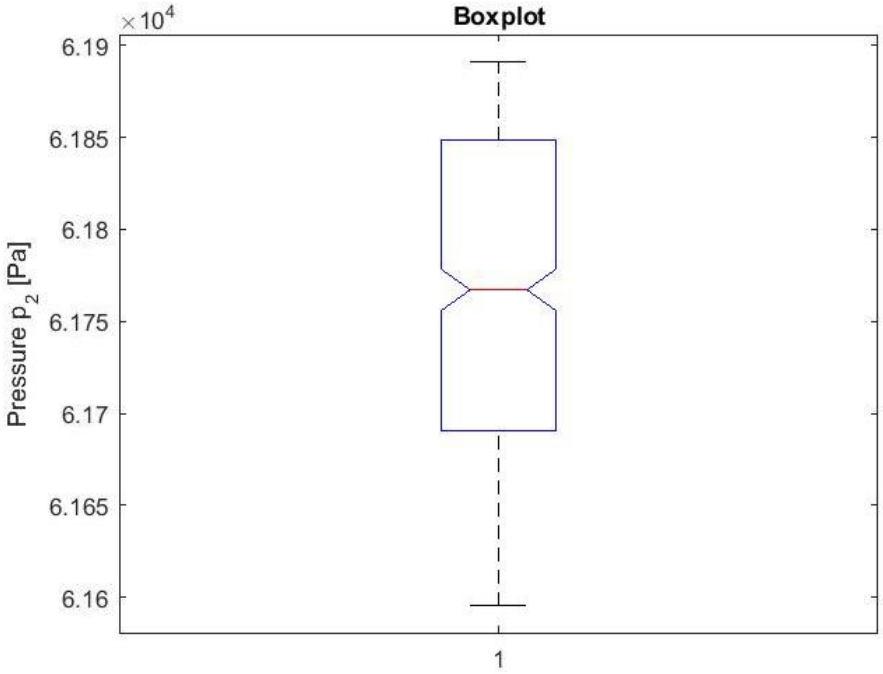

Figure 55. Boxplot of data set of pressure p_2.

The red line in between the peaks of the notch marks the median value standing at 61767 Pa. The lower blue edge of the box labels the 25th quantile equal to 61691 Pa and the upper blue edge labels the 75th quantile equal to 61849 Pa. The whiskers extends to the farthest data that are not considered outliers. No red sign marks are present implying no outliners are present.

Graphical methods

Histogram is the most used and best known method of data visualization.

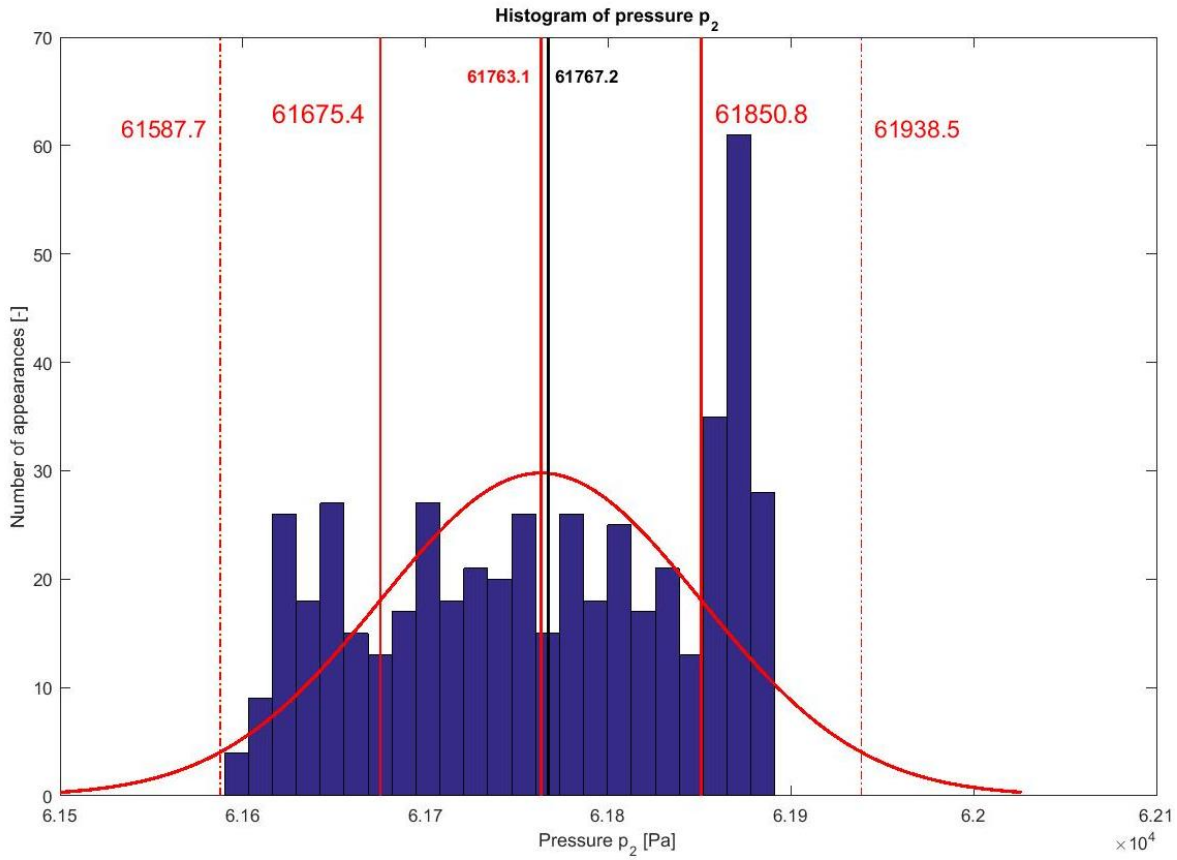

Figure 56. Histogram of pressure p_2.

The histogram roughly follows the Gaussian distribution (red curve). It shows there is a certain level of deviation from normal distribution. However, we can still consider it normal distribution regarding the statistics. The 500-sample data set is separated into 23 bins. The black vertical line in the middle marks up the median value. The red line besides marks up the mean value. The mean and median lines almost coincide which supports the idea of data normality. The two vertical lines on each side represent one standard deviation and statistically 68 % of all data. The two dashed lines on each side represent two standard deviations and statistically 95 % of all data. The data set has negative skewness and platykurtic distribution.

Another way to graphically show data similarity to normal distribution is a P-P diagram. Cumulative distribution function of data set in blue is compared with a cumulative distribution function of normal distribution in black. The more the two distributions overlap, the better normality the data set has.

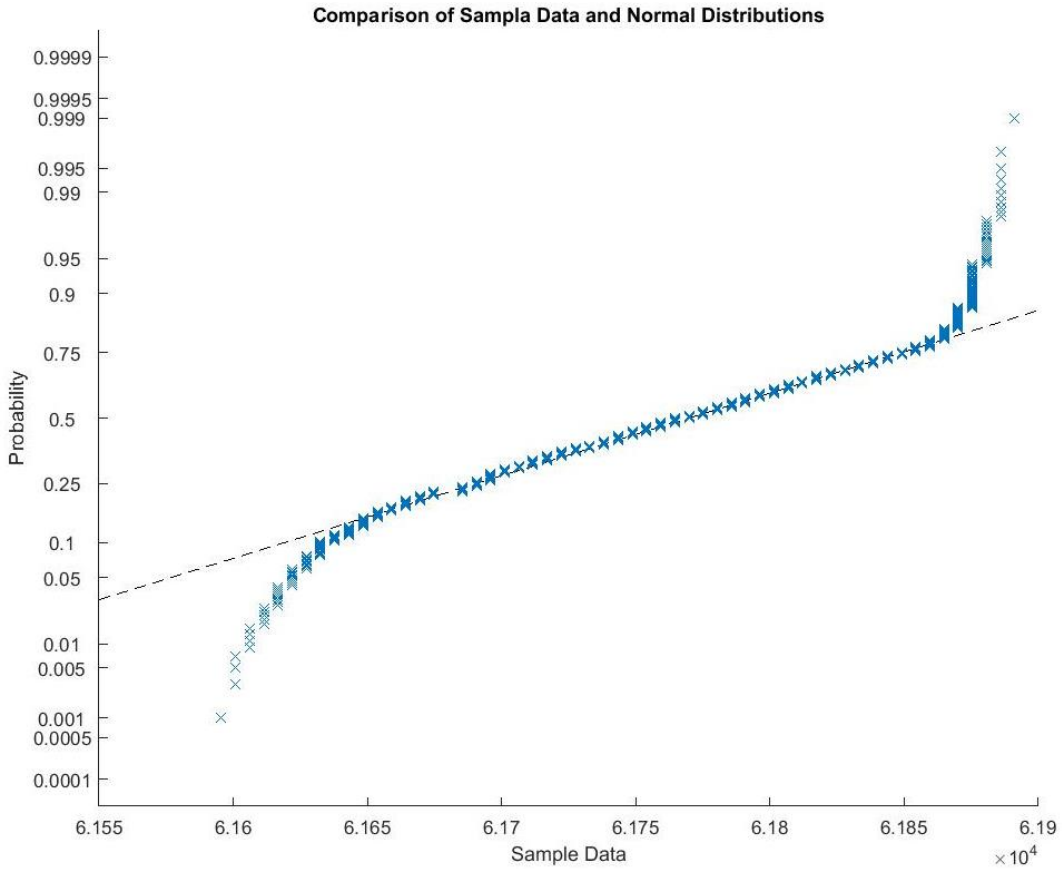

Figure 57. PP Plot of the sample data distribution versus normal distribution.

The blue crosses copy sufficiently enough the black line of normal distribution. The middle portion matches almost perfectly. The ends peel off quite significantly, which indicates certain deviation from normal distribution. Overall, we can assume the sample data distribution is rather normal.

Similar to the P-P diagram, the Q-Q diagram also shows the comparison of measured and theoretical distribution. Q-Q stands for 'quantile-quantile' diagram. A quantile from a data set and a quantile of normal distribution stand against each other. The red line symbolizes the normal distribution quantile and the blue crosses symbolize the quantile of the data set distribution. The closer the crosses are to the red line, the more the data set's distribution corresponds to normal.

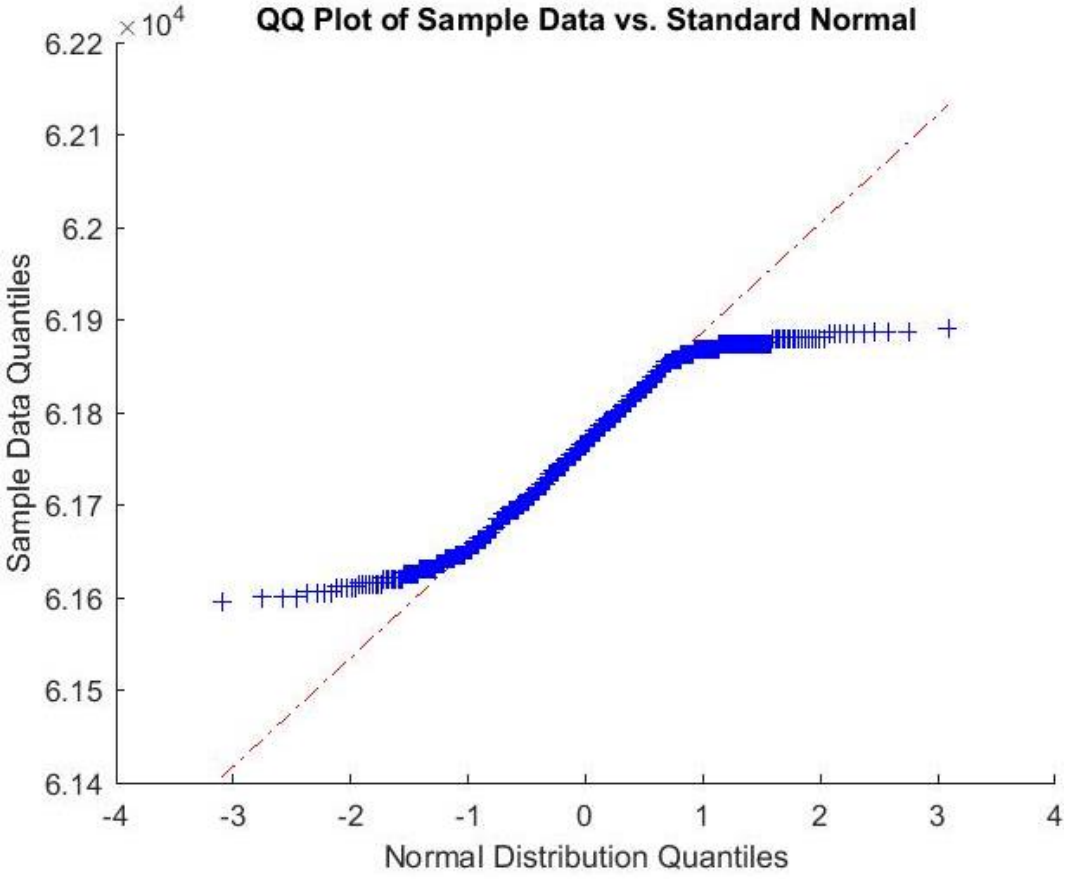

Figure 58: QQ plot of sample data quantiles versus normal distribution quantiles.

Blue crosses of sample data quantiles follow in the middle the red line of normal distribution. Both ends are affected in the same fashion, as is the case for PP plot. The ends veer off the normal distribution. This again signalizes that the sample data do not match completely the normal distribution. Overall, the match seems satisfactory and therefore we rule the sample data distribution normal.

14 Conclusion

Due to expansion of the steam in the turbine, the quality of steam drops and water content is present. Steam is no longer a one-phase medium, however, two-phase and becomes something what we call wet steam. The water droplets negatively affect mainly the rotor blades and the stator blades and therefore it is important to know the wet steam water content.

IAPWS IF-97 tables are used for determination of speed of sounds in the two-phase region. The input variables are static pressure p_S and quality of steam x. Spectrometric probes are used during the measurement to acquire data about the quality of steam. The overall quality of steam is given below.

Quality of steam x in front of the blade reaches: $x = 90.5 \div 94\ \%$

Quality of steam x behind the blade reaches: $x = 85 \div 91\ \%$

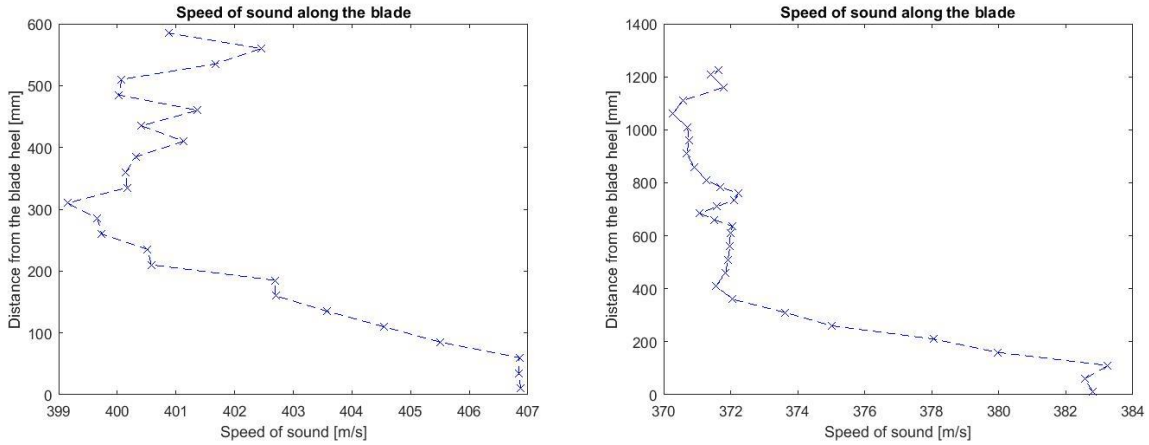

Speed of sound in the front and behind the blade.

To estimate properly the static, dynamic and total pressures in the turbine, we need to know the characteristic of the probe given by calibration coefficients and calibration equations. The calibration is done at a wind tunnel in Doosan Škoda Power R&D Centre.

Calibration coefficient $k_{\varepsilon 32}$ is selected because it delivers the best results over different intervals, is monotonous with relatively gradual slope, and no discontinuations and inflection points are present. A quadratic polynomial, given below, approximates its progress.

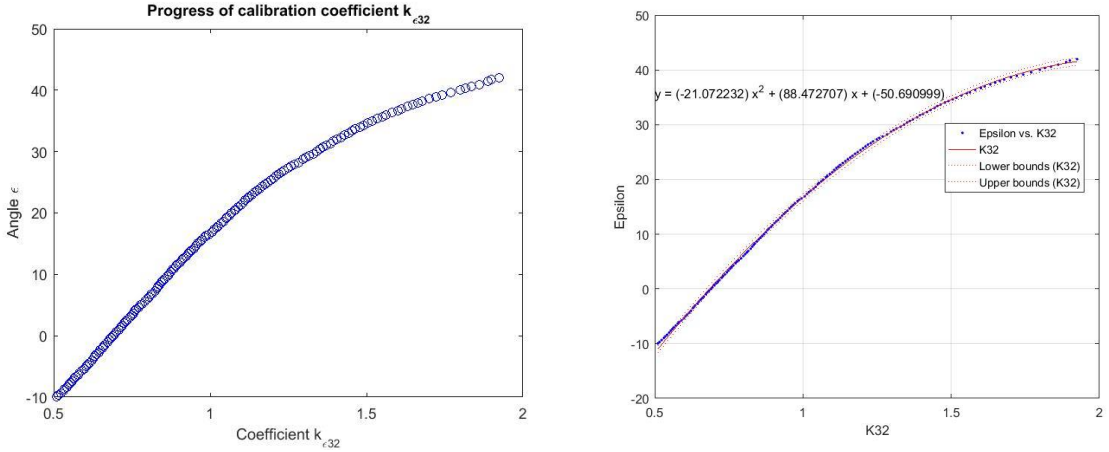

Calibration coefficients $k_{\varepsilon 32}$ and its calibration equation.

Coefficient	x^2	x^1	x^0
K_{32}	**-21.07**	**88.47**	**-50.69**

With use of reference Pitot-static probe, we determine the calibration coefficients for static and dynamic pressures. The flattest parts of curves are chosen, for they have the lowest sensitivity towards error, in case the calculated angle ε slightly varies from the true value.

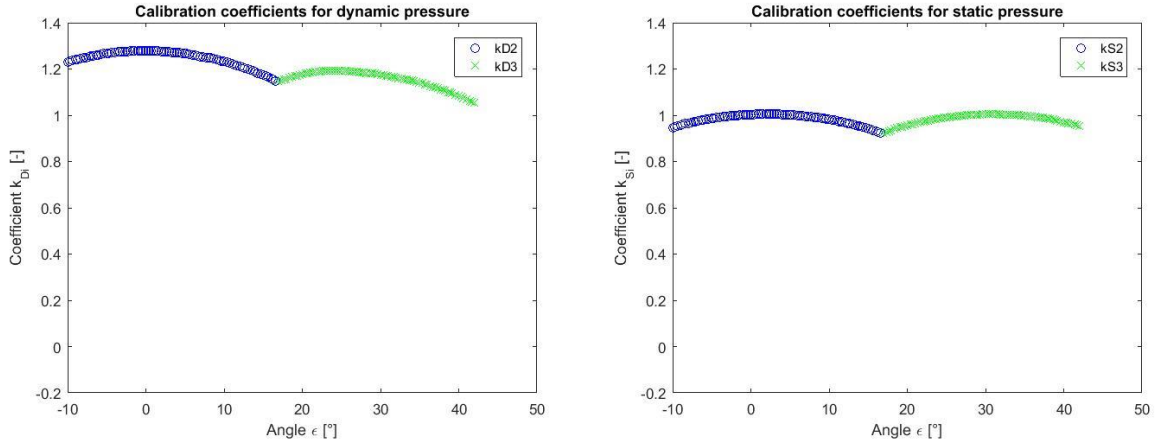

Calibration equations for of both coefficients are given in table here:

Coefficient	**ε Interval**	x^4	x^3	x^2	x^1	x^0
k_{D2}	⟨-10°, 16.52°⟩	$-1.91*10^{-7}$	$2.68*10^{-6}$	$-4.53*10^{-4}$	$-1.43*10^{-4}$	1.28
k_{D3}	(16.52°, 42°⟩	$-8.25*10^{-7}$	$1.10*10^{-4}$	$-5.45*10^{-3}$	$1.24*10^{-1}$	$1.52*10^{-1}$
k_{S2}	⟨-10°, 16.52°⟩	$-2.45*10^{-7}$	$3.79*10^{-6}$	$-3.66*10^{-4}$	$1.38*10^{-3}$	1.00
k_{S3}	(16.52°, 42°⟩	$-1.62*10^{-7}$	$1.85*10^{-5}$	$-1.18*10^{-3}$	$3.90*10^{-2}$	$5.26*10^{-1}$

Calibration coefficients and their equations are used for calculation of angle ε from the measured data. The 7-hole probe cannot tilt when collecting data in the turbine, therefore we use the calibration equation $k_{\varepsilon 32}$ to estimate the angle ε. Calibration equations k_D and k_S to estimate the real coefficients k_D and k_S and with these also calculate the static, dynamic and total pressures.

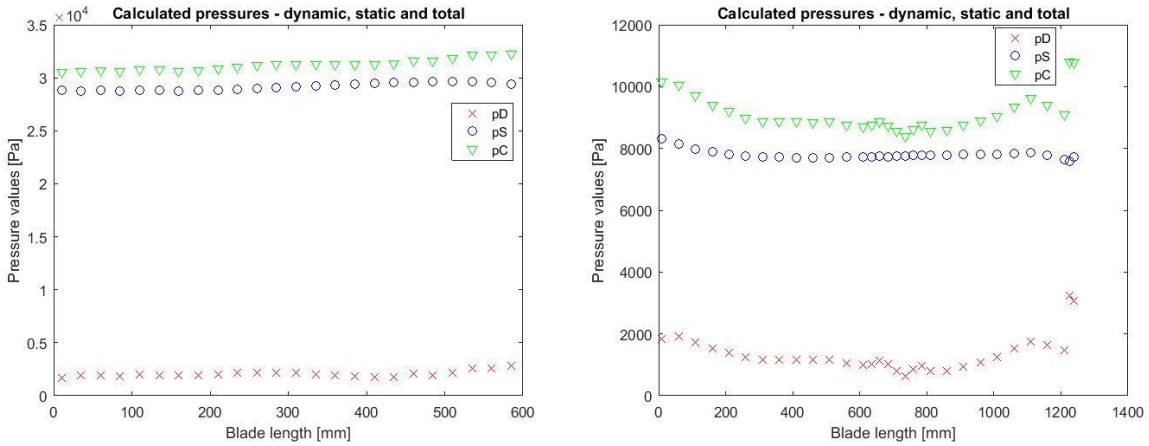

Calculated total, dynamic and static pressures in the front and back of the blade.

Those pressures and thermodynamic table IAPWS IF-97 are used to calculate the steam velocity c.

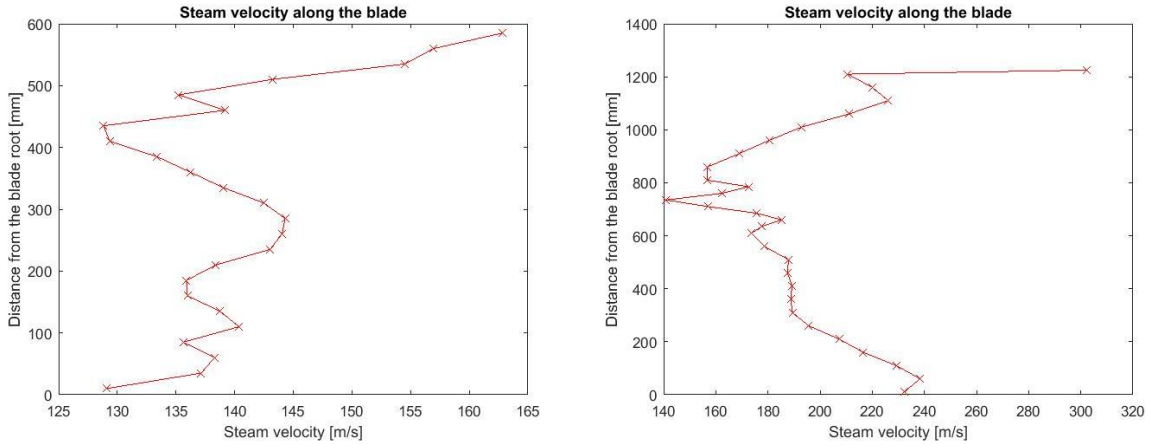

Steam velocity develpment along the blade length. In front of [left] and behind [right] the blade.

Speed in front of the blade ranges from 129 to 163 m/s.

Speed behind the blades ranges from 141 to 238 m/s.

No measurement is 100% accurate and therefore all the measurements have to be taken with a sense of skepticism. We denote the skepticism mathematically as an uncertainty or confidence bounds, resp. Expanded uncertainties of the pressure measurement are shown in table below.

Pressure	Expanded uncertainty in the front of the blade [Pa]	Expanded uncertainty in the back of the blade [Pa]
p_b	144.90	144.90
p_B	310.49	310.40
p_2	310.58	310.62
p_3	310.82	310.14

The calculated dynamic and static pressures and their absolute and relative uncertainties are given in the table below.

In front of the blade				Behind the blade			
Dynamic pressure uncertainty		Static pressure uncertainty		Dynamic pressure uncertainty		Static pressure uncertainty	
Absolute	Relative	Absolute	Relative	Absolute	Relative	Absolute	Relative
19.7 Pa	**0.937 %**	**455.4 Pa**	**1.760 %**	**22.1 Pa**	**1.08 %**	**465.3 Pa**	**5.416 %**

The static and dynamic pressures are used to determine different components of speeds depicted in the fig. 13 . Table below records the results of absolute and relative uncertainties.

Steam component	Expanded uncertainty in the front of the blade		Expanded uncertainty in the back of the blade	
	Δy	Relative	Δy	Relative
c	1.26 m/s	**0.792 %**	6.85 m/s	**2.29 %**
c_u	0.417 m/s	**0.814 %**	3.81 m/s	**2.33 %**
c_z	1.18 m/s	**0.796 %**	5.68 m/s	**2.92 %**
c_r	0.458 m/s	**0.796 %**	4.08 m/s	**2.34 %**

In the graphs is the uncertainty drawn as an interval in between two lines where the real speed could locate with 95 % accuracy. Picture here shows the upper and lower boundary of the confidence interval for steam velocity c.

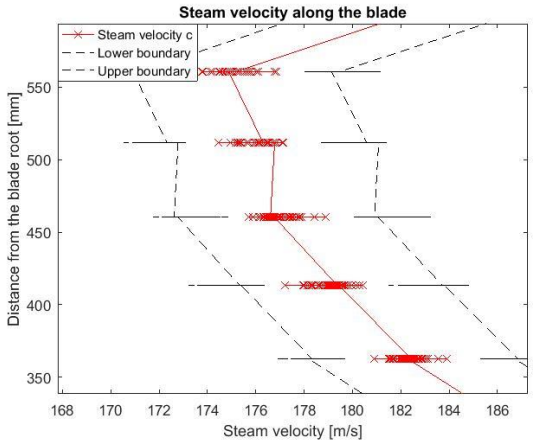

Exploratory analysis of one-dimensional data provides the information what data set we are dealing with. EDA helps us to prove or disprove whether the measured data comply with normal distribution. EDA results show in favor of normal distribution. No trends or periodic intervals are present, supporting normal distribution. Graphical methods, especially histograms, are common tools to easily check the data distribution against normal distribution.

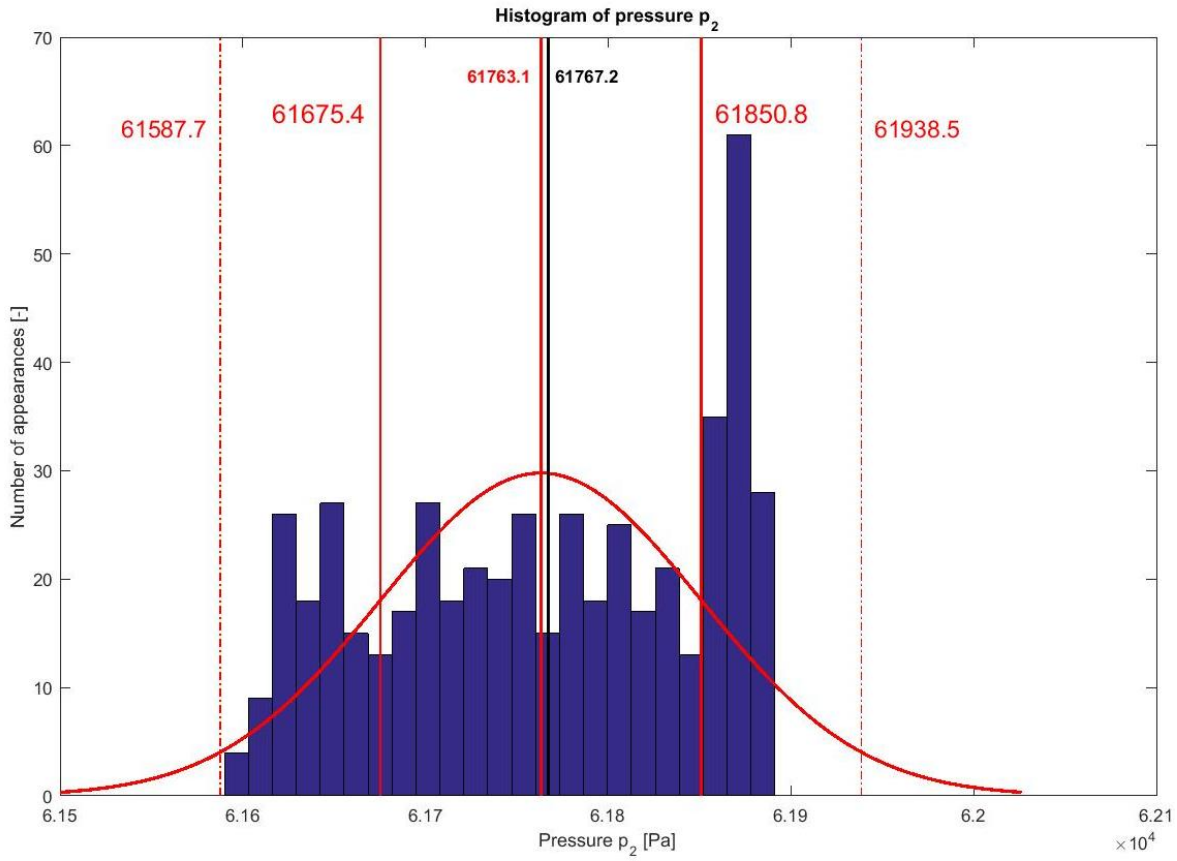

Data set for pressure p_2 has roughly Gaussian distribution. Mean (61763.1) and median (61767.2) do not coincide, however, they are very close to each other, which supports compliance of the data with normal distribution. Skewness of the distribution is negative, because the longer tail stretches to the left. Data set is more of platykurtic distribution than mesokurtic. All the data are located within ±2σ. Overall, we can claim the data set has rather normal distribution; therefore, they are suitable for further calculations.

The calculated steam velocities, static and dynamic pressures, quality of steam can be further used to calculate other thermodynamic properties using the IAPWS IF-97 steam tables and thermodynamic formulas. Such as static, dynamic or total enthalpies, enthalpy drops in stages, change in entropy, stage reaction number, rotor and stator efficiency and loss, speed ratios, stage efficiency, absolute and relative velocity of steam coming at a blade or leaving it, angles of the steam hitting/leaving the blade, velocity of gaseous and liquid phase, stagnation temperature or steam flowrate. Results from the thesis may be compared to the turbine designed properties. In case they do significantly differ, amendments in the algorithms of numerical models are to be carried out.

15 Figures, tables, formulas

15.1 Figures

Fig. 1 4
Fig. 2 6
Fig. 3 6
Fig. 4 7
Fig. 5 8
Fig. 6 8
Fig. 7 8
Fig. 8 9
Fig. 9 9
Fig. 10 10
Fig. 11 10
Fig. 12 12
Fig. 13 13
Fig. 14 14
Fig. 15 14
Fig. 16 14
Fig. 17 15
Fig. 18 16
Fig. 19 16
Fig. 20 17
Fig. 21 18
Fig. 22 19
Fig. 23 19
Fig. 24 20
Fig. 25 20
Fig. 26 21
Fig. 27 23
Fig. 28 26
Fig. 29 ..... 31, 56
Fig. 30 ..... 32, 56
Fig. 31 33
Fig. 32 36
Fig. 33 36
Fig. 34 37
Fig. 35 38
Fig. 36 38
Fig. 37 39
Fig. 38 39
Fig. 39 40
Fig. 40 41
Fig. 41 41
Fig. 42 42
Fig. 43 43

Fig. 44 46
Fig. 45 47
Fig. 46 47
Fig. 47 48
Fig. 48 48
Fig. 49 49
Fig. 50 49
Fig. 51 52
Fig. 52 53
Fig. 53 54
Fig. 54 57
Fig. 55 57
Fig. 56 58
Fig. 57 59
Fig. 58 60

15.2 Tables

Table 1 15
Table 2 34
Table 3 42
Table 4 42
Table 5 43
Table 6 44
Table 7 44
Table 8 51
Table 9 53

15.3 Formulas

Formula 1 11
Formula 2 11
Formula 3 11
Formula 4 12
Formula 5 12
Formula 6 12
Formula 7 12
Formula 8 13
Formula 9 13
Formula 10 13
Formula 11 13
Formula 12 13
Formula 13 15
Formula 14 16
Formula 15 21
Formula 16 21
Formula 17 21
Formula 18 22
Formula 19 22
Formula 20 27
Formula 21 27
Formula 22 27
Formula 23 28
Formula 24 29
Formula 25 29
Formula 26 29
Formula 27 29
Formula 28 29
Formula 29 29
Formula 30 30
Formula 31 31
Formula 32 31
Formula 33 32
Formula 34 32
Formula 35 32
Formula 36 33
Formula 37 33
Formula 38 33

16 References

[1] Bell, S., 2001. *Measurement Good Practice Guide No. 11 (Issue 2) - A Beginner's Guide to Uncertainty of Measurement.* [pdf] Available at: <https://www.dit.ie/media/physics/documents/GPG11.pdf > [Accessed 8 June 2020]

[2] Chaluš, M., 2013. *Development of a tool for control and support of evaluation of experiments in a medium-speed wind tunnel.* (Original title: Vývoj nástroje pro řízení a podporu vyhodnocení experimentů ve středněrychlostním aerodynamickém tunelu). [online] Available at: <https://portal.zcu.cz/portal/studium/prohlizeni.html> [Accessed 8 June 2020].

[3] CRAIC Technologies, 2019. *Ultraviolet-visible-near infrared Spectrophotometry* [online] Available at: <http://www.microspectra.com/technical-support/248-spectrophotometer-design> [Accessed 8 June 2020]

[4] Engineering Statistics Handbook, 2020. *Measures of Location.* [online] Available at: <https://www.itl.nist.gov/div898/handbook/eda/section3/eda351.htm> [Accessed 8 June 2020]

[5] Engineering Statistics Handbook, 2020. *Measures of Scale*. [online] Available at: <https://www.itl.nist.gov/div898/handbook/eda/section3/eda356.htm> [Accessed 8 June 2020]

[6] Engineering Statistics Handbook, 2020. *Measures of Skewness and Kurtosis*. [online] Available at: <https://www.itl.nist.gov/div898/handbook/eda/section3/eda35b.htm> [Accessed 8 June 2020]

[7] IAPWS Org., 2018. *Main IAPWS Thermodynamic Property Formulations*. [online] Available at: <http://www.iapws.org/newform.html> [Accessed 8 June 2020].

[8] Kochurov, R., 2017. *Rotor Heating Conditions Influence on the Thermostructural State and Lifetime of the 325 MW Steam Turbine During Start-Ups.* [online] Available at: <https://www.researchgate.net/figure/325-MW-Steam-Turbine-HP-Cylinder-Cross-Section-Thermo-structural-Analysis-Cold-start-up_fig1_321839162> [Accessed 9 June 2020]

[9] Kolovratník, M., 2016. *Research and developmental measurements of wet steam liquid phase in the ETE steam turbine* (Original title: Výzkumná a vývojová měření kapalné fáze mokré páry v parní turbíně ETE). Research report No. Z-596/2016. Property of CTU in Prague.

[10] MathWorks, 2020. *Quantile-quantile plot*. [online] Available at: <https://www.mathworks.com/help/stats/qqplot.html> [Accessed 9 June 2020].

[11] MathWorks, 2020. *Probability plots.* [online] Available at: <https://www.mathworks.com/help/stats/probplot.html#:~:text=probplot(%20y%20)%20creates%20a%20normal,that%20represents%20the%20theoretical%20distribution.> [Accessed 9 June 2020].

[12] Meloun, M., Militký, J., 2004. Statistical Analysis of experimental data. (Original title: Statistická analýza experimentálních dat). Prague:ACADEMIA

[13] Nex Instrument, 2020. *Rosemount 3051*. [online] Available at: <https://www.nexinstrument.com/3051TG4A2B21AB4E5D4M5T1Q4S5HR5+0306RT22BA11> [Accessed 8 June 2020].

[14] Sedlák, K., Hoznedl, M., Tajč, L., 2013. *Revision of calibration equation of a probe used for flow measurement in two phase environment of turbomachinery*. (Original title: Revize kalibračních rovnic sondy používané pro měření v prostředí dvoufázového proudění lopatkových strojů). Technical report No. TZTP 0868a. Property of Doosan Škoda Power s.r.o., Pilsen.

[15] Sedlák, K., 2016. *Calibration, measurement on a turbine with a 7-hole pneumatic probe and primary data processing.* (Original title: Kalibrace, měření na díle a vyhodnocení primárních dat měřených diskovou sedmiotvorovou pneumatickou sondou). Research report No. VZTP 1113. Property of Doosan Škoda Power s.r.o., Pilsen.

[16] Sedlák, K., 2017. *Statistical processing of experimentally acquired primary data.* (Original title: Statistické zpracování experimentálně získaných primárních dat). Research report No. VZTP 1131. Property of Doosan Škoda Power s.r.o., Pilsen.

[17] Taylor, C., 2019. *What is Skewness in Statistics?*. [online] Available at: <https://www.thoughtco.com/what-is-skewness-in-statistics-3126242> [Accessed 8 June 2020]

[18] Taylor, C., 2019. *How to Classify the Kurtosis of Distributions*. [online] Available at: <https://www.thoughtco.com/what-is-kurtosis-3126241> [Accessed 8 June 2020]

[19] Woodford, Ch., 2019. *Steam turbines*. [online] Available at: <https://www.explainthatstuff.com/steam-turbines.html> [Accessed 7 June 2020].

17 Appendix

MATLAB scripts